ReGeo
ISSN: 2177-3246

SEASONAL AND LAND USE INTERACTION ON WATER QUALITY IN THE CAMPO ALEGRE STREAM, GOIANO CERRADO: EVIDENCE OF URBAN IMPACT

INTERAÇÃO SAZONAL E USO DO SOLO NA QUALIDADE DA ÁGUA DO RIBEIRÃO CAMPO ALEGRE, CERRADO GOIANO: EVIDÊNCIAS DE IMPACTO URBANO

INTERACCIÓN ESTACIONAL Y USO DEL SUELO EN LA CALIDAD DEL AGUA DEL ARROYO CAMPO ALEGRE, CERRADO DE GOIÁS: EVIDENCIAS DE IMPACTO URBANO

https://doi.org/10.56238/revgeov17n10-209

Data de submissão: 28/09/2026 **Data de publicação:** 28/10/2026

Emanuelly de Oliveira Mecenas[1], Layara Alexandre Bessa[2], Galileu Silva[3], Luciana Cristina Vitorino[4]

ABSTRACT

Freshwater ecosystems in the Brazilian Cerrado face escalating degradation from agricultural expansion and urban growth. Understanding the synergistic interaction between land use and seasonal hydrological pulses is critical for water resource management. This study evaluated the spatial-temporal dynamics of water quality and potential ecotoxicological risks in the Campo Alegre Stream basin (Santa Helena de Goiás, Brazil). Water samples were collected across three land-use zones - Conservation Unit, Agricultural Area, and Urban Area - during the Rainy Season and Dry Season of 2023. Twenty-six physicochemical, optical, metallic, and microbiological parameters were analyzed according to standard methodologies. Statistical evaluations included two-way ANOVA with Tukey's post-hoc test, Pearson correlation, Hierarchical Cluster Analysis (HCA), and the calculation of the Water Quality Index (WQI). Compliance was assessed against CONAMA Resolution No. 357/2005 Class 2 standards. Seasonal rainfall-driven runoff degraded water clarity and elevated metal concentrations during the Rainy Season, with Turbidity (mean of 189.33 NTU), Aluminium (mean of 0.15 mg L^{-1}), and Manganese (mean of 0.10 mg L^{-1}) exceeding regulatory thresholds. The Urban Area exhibited chronic microbial and organic contamination, consistently breaching limits for *Escherichia coli* (up to 4.41 $\log_{10}$ MPN 100 mL^{-1}) and Biochemical Oxygen Demand (BOD, mean of 4.70 mg L^{-1}) across both seasons. Total Hardness, Total Dissolved Solids (TDS), Electrical Conductivity (EC), and Nitrate increased substantially during the Dry Season due to reduced dilution. Pearson correlation and HCA grouped samples primarily by seasonality and secondarily by land use. The WQI classified the Conservation Unit and Agricultural Area from "Good" (62.5–69.8) in the Rainy Season to "Good"/"Excellent" (77.2–79.2) in the Dry Season, whereas the Urban Area remained deteriorated at the "Good/Moderate" border (~52.0) year-round. Stormwater runoff from highly weathered Cerrado soils coupled with urban surface washing drives seasonal spikes in particulate matter and bioactive metals, posing toxicological risks to aquatic biota.

[1] Master's Degree in Biodiversity and Conservation. Instituto Federal Goiano – campus Rio Verde.
E-mail: emanuelly.mecenas@estudante.ifgoiano.edu.br
[2] PhD in Agronomy. Instituto Federal Goiano – campus Rio Verde.
E-mail: layara.bessa@ifgoiano.edu.br
[3] Master's Degree in Applied Engineering and Sustainability. Instituto Federal Goiano – campus Rio Verde.
E-mail: galileu.silva@estudante.ifgoiano.edu.br
[4] PhD in Genetics and Molecular Biology. Instituto Federal Goiano – campus Rio Verde.
E-mail: luciana.vitorino@ifgoiano.edu.br

Persistent urban non-compliance highlights untreated domestic sewage discharge that overrides natural river self-purification. Low Phosphorus levels (<0.03 mg L^{-1}) currently prevent severe eutrophication despite high Nitrate availability. Water quality in the Campo Alegre basin is governed by the interplay between seasonal hydrological pulses and chronic urban pollution. Urban pressures continuously degrade the stream beyond regulatory limits for Class 2 waters, emphasizing the urgent need for expanded municipal wastewater treatment and agricultural soil conservation practices.

Keywords: Water Quality Index (WQI). Urban Runoff. Ecotoxicology. Cerrado Streams. Seasonal Variability.

RESUMO

Os ecossistemas de água doce no Cerrado brasileiro enfrentam uma degradação crescente decorrente da expansão agrícola e do crescimento urbano. Compreender a interação sinérgica entre o uso do solo e os pulsos hidrológicos sazonais é fundamental para a gestão dos recursos hídricos. Este estudo avaliou a dinâmica espaço-temporal da qualidade da água e os potenciais riscos ecotoxicológicos na bacia do Córrego Campo Alegre (Santa Helena de Goiás, Brasil). Amostras de água foram coletadas em três zonas de uso do solo — Unidade de Conservação, Área Agrícola e Área Urbana — durante as estações chuvosa e seca de 2023. Vinte e seis parâmetros físico-químicos, ópticos, metálicos e microbiológicos foram analisados seguindo metodologias padrão. As avaliações estatísticas incluíram ANOVA de dois fatores com teste *post-hoc* de Tukey, correlação de Pearson, Análise de Agrupamento Hierárquico (AAH) e o cálculo do Índice de Qualidade da Água (IQA). A conformidade foi avaliada com base nos padrões da Classe 2 da Resolução CONAMA nº 357/2005. O escoamento superficial induzido pelas chuvas sazonais comprometeu a transparência da água e elevou as concentrações de metais durante a estação chuvosa, com a turbidez (média de 189,33 NTU), o alumínio (média de 0,15 mg L^{-1}) e o manganês (média de 0,10 mg L^{-1}) ultrapassando os limites regulatórios. A Área Urbana apresentou contaminação microbiana e orgânica crônica, excedendo consistentemente os limites para *Escherichia coli* (até 4,41 $\log_{10}$ NMP 100 mL^{-1}) e Demanda Bioquímica de Oxigênio (DBO; média de 4,70 mg L^{-1}) em ambas as estações. A dureza total, os sólidos dissolvidos totais (SDT), a condutividade elétrica (CE) e o nitrato aumentaram substancialmente durante a estação seca, devido à menor diluição. A correlação de Pearson e a AAH agruparam as amostras, primariamente, pela sazonalidade e, secundariamente, pelo uso do solo. O IQA classificou a Unidade de Conservação e a Área Agrícola como "Bom" (62,5–69,8) na estação chuvosa e como "Bom"/"Excelente" (77,2–79,2) na estação seca; por outro lado, a Área Urbana permaneceu em estado deteriorado, na transição entre "Bom" e "Moderado" (~52,0), ao longo de todo o ano. O escoamento superficial de águas pluviais em solos do Cerrado altamente intemperizados, somado à lavagem de superfícies urbanas, provoca picos sazonais de material particulado e metais bioativos, gerando riscos toxicológicos para a biota aquática. A persistente falta de conformidade em áreas urbanas evidencia o lançamento de esgoto doméstico sem tratamento, o que sobrepuja a capacidade natural de autodepuração dos rios. Atualmente, os baixos níveis de fósforo (<0,03 mg L^{-1}) evitam uma eutrofização severa, apesar da alta disponibilidade de nitrato. A qualidade da água na bacia do Campo Alegre é determinada pela interação entre pulsos hidrológicos sazonais e a poluição urbana crônica. As pressões urbanas degradam continuamente o curso d'água, ultrapassando os limites regulatórios estabelecidos para águas de Classe 2, o que ressalta a necessidade urgente de ampliar o tratamento de esgoto municipal e adotar práticas de conservação do solo na agricultura.

Palavras-chave: Índice de Qualidade da Água (IQA). Escoamento Superficial Urbano. Ecotoxicologia. Riachos do Cerrado. Variabilidade Sazonal.

RESUMEN
Los ecosistemas de agua dulce en el Cerrado brasileño enfrentan una degradación creciente debido a la expansión agrícola y el crecimiento urbano. Comprender la interacción sinérgica entre el uso del suelo y los pulsos hidrológicos estacionales es fundamental para la gestión de los recursos hídricos. Este estudio evaluó la dinámica espacio-temporal de la calidad del agua y los posibles riesgos ecotoxicológicos en la cuenca del arroyo Campo Alegre (Santa Helena de Goiás, Brasil). Se recolectaron muestras de agua en tres zonas según el uso del suelo —unidad de conservación, área agrícola y área urbana— durante las temporadas de lluvias y de sequía de 2023. Se analizaron veintiséis parámetros fisicoquímicos, ópticos, metálicos y microbiológicos siguiendo metodologías estandarizadas. Las evaluaciones estadísticas incluyeron un análisis de varianza (ANOVA) de dos factores con la prueba *post-hoc* de Tukey, correlación de Pearson, análisis de conglomerados jerárquicos (HCA, por sus siglas en inglés) y el cálculo del Índice de Calidad del Agua (ICA). El cumplimiento normativo se evaluó conforme a los estándares de la Clase 2 de la Resolución CONAMA n.º 357/2005. La escorrentía generada por las precipitaciones estacionales redujo la claridad del agua y aumentó las concentraciones de metales durante la temporada de lluvias; la turbidez (promedio de 189,33 NTU), el aluminio (promedio de 0,15 mg L^{-1}) y el manganeso (promedio de 0,10 mg L^{-1}) superaron los umbrales normativos. El área urbana presentó una contaminación microbiana y orgánica crónica, superando sistemáticamente los límites establecidos para *Escherichia coli* (hasta 4,41 $\log_{10}$ NMP 100 mL^{-1}) y la demanda bioquímica de oxígeno (DBO; promedio de 4,70 mg L^{-1}) en ambas temporadas. La dureza total, los sólidos disueltos totales (SDT), la conductividad eléctrica (CE) y los nitratos aumentaron considerablemente durante la temporada de sequía debido a una menor dilución. La correlación de Pearson y el HCA agruparon las muestras principalmente según la estacionalidad y, en segundo lugar, según el uso del suelo. El ICA clasificó a la unidad de conservación y al área agrícola en un rango de «bueno» (62,5–69,8) durante la temporada de lluvias, pasando a «bueno/excelente» (77,2–79,2) en la temporada de sequía; por el contrario, el área urbana permaneció en un estado deteriorado, situándose en el límite entre «bueno» y «moderado» (~52,0) durante todo el año. La escorrentía pluvial proveniente de suelos altamente meteorizados del Cerrado, sumada al lavado de superficies urbanas, provoca picos estacionales de material particulado y metales bioactivos, lo que conlleva riesgos toxicológicos para la biota acuática. El persistente incumplimiento de la normativa en áreas urbanas pone de manifiesto el vertido de aguas residuales domésticas sin tratar, el cual supera la capacidad natural de autodepuración de los ríos. Los bajos niveles de fósforo (<0,03 mg L^{-1}) evitan, por el momento, una eutrofización severa, a pesar de la elevada disponibilidad de nitratos. La calidad del agua en la cuenca de Campo Alegre está determinada por la interacción entre los pulsos hidrológicos estacionales y la contaminación urbana crónica. Las presiones urbanas degradan continuamente el curso de agua, superando los límites normativos establecidos para aguas de Clase 2; esto subraya la urgente necesidad de ampliar el tratamiento de aguas residuales municipales e implementar prácticas de conservación de suelos agrícolas.

Palabras clave: Índice de Calidad del Agua (ICA). Escorrentía Urbana. Ecotoxicología. Arroyos del Cerrado. Variabilidad Estacional.

1 INTRODUCTION

Freshwater is an indispensable natural resource for ecosystem maintenance, public health, and sustainable socioeconomic development on a global scale (Bănăduc *et al.,* 2022; Apostolaki *et al.,* 2020). In recent decades, rapid population growth, unplanned urbanization, and the expansion of agricultural activities have intensified both quantitative and qualitative pressures on surface water resources (Mishra, 2023). The degradation of water quality compromises water security, triggers severe ecotoxicological implications for aquatic biota, increases treatment costs for human consumption, and amplifies the risk of waterborne disease outbreaks (Mishra *et al.,* 2021; Damania *et al.,* 2019). In this scenario, continuous monitoring and understanding the key drivers of water quality across watersheds become priority strategic tools for environmental management and the formulation of effective public policies (Chapman, 2021).

Currently, it is well established in the literature that land use and climate variability are the main drivers affecting the physicochemical and microbiological characteristics of rivers and streams (Laniyan *et al.,* 2025; You *et al.,* 2019; Liang *et al.,* 2013). Studies in freshwater ecosystems demonstrate that urban areas act as point and nonpoint sources of chronic pollution, introducing heavy loads of domestic sewage, organic matter, and pathogens, as well as metals and emerging contaminants carried by runoff from impervious surfaces (Singh *et al.,* 2022; Wang *et al.,* 2020). Conversely, agricultural and conservation areas typically exhibit dynamics dependent on the seasonal hydrological pulse, in which surface runoff during the Rainy Season promotes the leaching of sediments and nutrients (Li *et al.,* 2023; Zahoor and Mushtaq, 2023), whereas the Dry Season favors the stabilization or concentration of certain dissolved ions. However, the extent to which seasonal variability can attenuate or intensify the impacts of anthropogenic contamination (Alkhadher *et al.,* 2025; Ayejoto *et al.,* 2023) across different land uses still presents nuances that require in-depth investigation.

Although the isolated effects of urbanization and agriculture on water bodies are widely documented (Cabrera *et al.,* 2023; Li *et al.,* 2023), a critical gap persists in scientific knowledge regarding the synergistic interaction between the seasonal pulse (Rainy Season vs. Dry Season) and the self-purification capacity of micro-basins subjected to continuous land-use gradients (conservation, agricultural, and urban). Research frequently focuses on point-in-time evaluations or isolated parameters (Yao *et al.,* 2024; Wang *et al.,* 2024; Wang *et al.,* 2023), neglecting the application of integrated multivariate statistical tools combined

with Water Quality Indices (WQI) (Uddin *et al.,* 2021) to diagnose how the contamination matrix restructures across seasons. Evidence in the literature indicates that the lack of integrated approaches limits the identification of early bioindicators of incomplete organic matter oxidation and heavy metal dynamics in tropical water bodies, where high temperatures and intense rainfall drastically alter biological reaction kinetics and metal ion solubility (Xiao *et al.,* 2024; Pinheiro *et al.,* 2021).

Additionally, there is a substantial literature gap regarding the quantification of ecotoxicological risks generated by the natural leaching of highly weathered tropical soils (such as Cerrado Oxisols) combined with urban effluents under slightly acidic pH fluctuations in the Rainy Season. In this context, the Campo Alegre Stream sub-basin features an urban section (municipality of Santa Helena de Goiás) located centrally within the sub-basin and expanding over several headwaters (Soares *et al.,* 2020), rendering water discharge and quality potentially vulnerable to unplanned urban expansion. Most regulatory studies conducted in this sub-basin rely solely on point compliance with regulatory thresholds (Rodrigues *et al.,* 2015), without evaluating how subtle physicochemical deviations exacerbate the bioaccumulation and chronic toxicity of metals such as free aluminum (Al^{3+}) and manganese (Mn) in aquatic communities. Given this uncertainty, it is hypothesized that seasonal variability acts as a modifying force on the water quality of the Campo Alegre Stream via diffuse sediment inputs during the Rainy Season, whereas in the urban stretch, chronic anthropogenic pressures override the river's natural self-purification dynamics, leading to continuous non-compliance with legal regulatory standards regardless of the season.

The state of Goiás stands out as an agro-industrial hub of major relevance in the Cerrado Biome, where intense land conversion for monocultures, high water extraction for irrigation, and urban expansion exert pressure on strategic supply sources (Queiroz *et al.,* 2026). Thus, the Campo Alegre Stream sub-basin exemplifies this spatial transition and water-use conflict, serving as a representative model for Cerrado freshwater ecosystems, where water extraction for irrigation and riparian vegetation removal near headwaters and Permanent Preservation Areas (APPs) are driving streamflow reduction (Soares *et al.,* 2020). To address this issue, this study aimed to evaluate water quality and the spatiotemporal dynamics of contaminants in the Campo Alegre Stream Sub-basin. Specifically, it sought to: (i) analyze and compare physicochemical and bacteriological parameters across a land-use gradient (Conservation Unit, Agricultural Area, and Urban Area); (ii) determine the influence of the seasonal hydrological pulse (Rainy Season and Dry Season) on these parameters;

and (iii) evaluate compliance with standards established by CONAMA Resolution No. 357/2005 (CONAMA, 2005) for Class 2 waters and bathing standards.

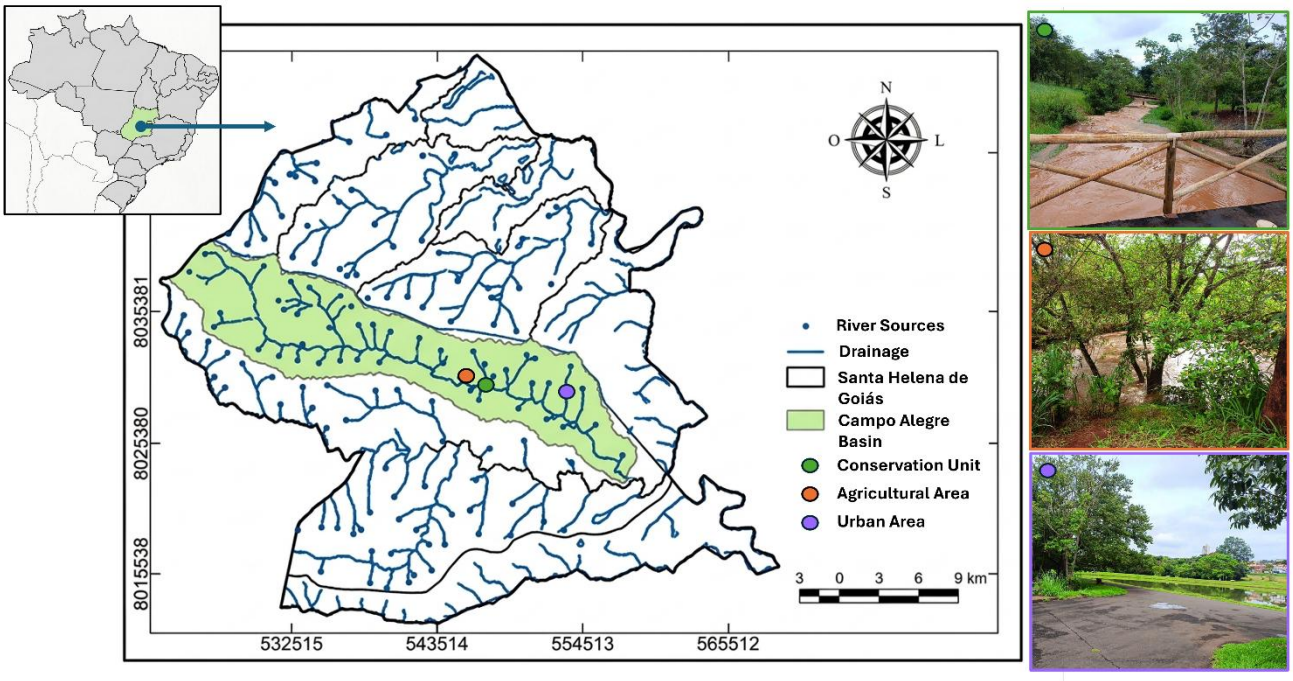
2 MATERIAL AND METHODS

2.1 STUDY AREA CHARACTERIZATION AND SAMPLING

The study was conducted in the Campo Alegre Stream sub-basin, located entirely in the municipality of Santa Helena de Goiás – GO, Brazil. This stream originates at coordinates 17º44’34”S and 50°45’44”W and empties into the São Tomás River (17º53’00”S and 57º27’12”W), with its sub-basin covering a drainage area of 14,363.7 ha (Rodrigues et al., 2015) (Figure 1). Sampling points influenced by different land-use profiles were selected along the stream and categorized into three locations: within a Municipal Conservation Unit (Turmim Azevedo Municipal Park - 17°48’2”S and 50°37’15”W, altitude 561 m), in an Agricultural Area upstream of the city (17°47’40”S and 50°38’1”W, altitude 567 m), and in an Urban Area (17°48’43”S and 50°35’33”W, altitude 541 m).

Figure 1

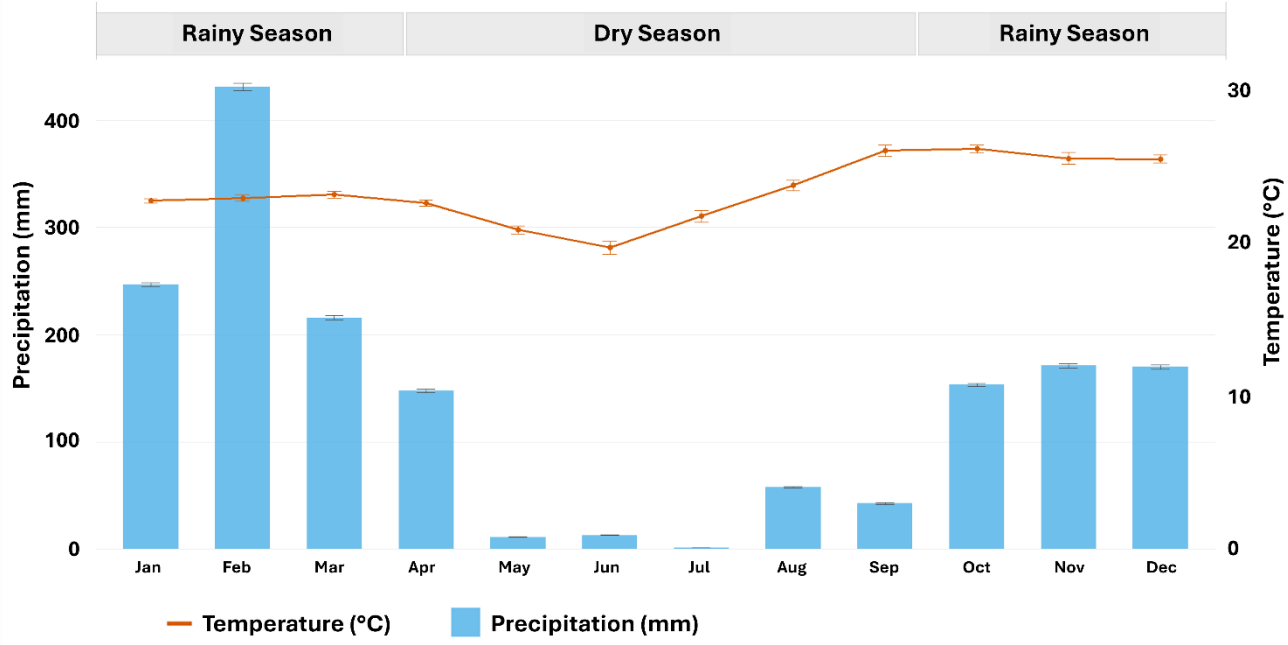
Location of the Campo Alegre Stream Basin in the municipality of Santa Helena de Goiás – GO, Brazil, and distribution of water sampling sites. Photos correspond to the respective sampling areas: Conservation Unit, Agricultural Area, and Urban Area.



Samples were collected in March and August 2023, representing the Rainy Season and Dry Season, respectively. Climate data recorded for the Santa Helena de Goiás region (Rio Verde Meteorological Station – GO) during the collection months showed Total Precipitation of 215.8 mm and 57.8 mm for March and August, respectively, and Mean Temperatures of 23.1 °C and 23.8 °C (INMET, 2023).

Figure 2

Total Precipitation and Mean Temperature data in the Campo Alegre Stream Basin during the water sampling year. Sampling performed in March and August, representing the Rainy Season and Dry Season.



Sampling, preservation, and handling procedures strictly followed the standard normative guidelines described in the National Guide for Sample Collection and Preservation (CETESB, 2014) and *Standard Methods for the Examination of Water and Wastewater* (APHA, 2005). All physicochemical and microbiological analyses were processed at the Water Quality Control Laboratory of the local sanitation utility responsible for public water supply and sewage systems.

Measurements were performed in triplicate (n = 3) for each sampling location in each season, repeated three times throughout the same sampling day at 4-hour intervals. Thus, a single sample represented the mean of three observations. All field and laboratory bench

equipment underwent routine verification and calibration using certified standard reference solutions according to manufacturers' specifications.

2.2 IN SITU AND GENERAL PHYSICOCHEMICAL PARAMETERS

Immediately after in situ sampling, water temperature and ambient temperature were measured using a calibrated digital thermometer (°C) (Incoterm 7665). In the laboratory, optical and physicochemical parameters were determined via electrometric, titrimetric, and spectrophotometric methods:

- **pH:** Determined potentiometrically (pH units) using a calibrated benchtop pH meter (Digimed DM-220) with pH 4.0, 7.0, and 10.0 standard reference buffer solutions.
- **Electrical Conductivity (EC):** Measured with a digital conductivity meter (Digimed DM-30P) equipped with an automatic temperature-compensated conductivity cell, with results expressed in μS cm^{-1}.
- **Total Dissolved Solids (TDS):** Quantified indirectly by converting electrical conductivity values using an empirical conversion factor of 0.55, with results expressed in mg L^{-1}.
- **Turbidity:** Evaluated nefelometrically via light scattering using a digital turbidimeter (Hach 2100Q), expressed in Nephelometric Turbidity Units (NTU).
- **Apparent Color:** Determined via colorimetric comparison using a Policontrol Aqua color meter, expressed in Color Units (CU).
- **Total Fluoride:** Measured potentiometrically using a fluoride ion-selective electrode (Thermo Scientific Orion 9609BNWP), expressed in mg F^- L^{-1}.

Titrimetric Parameters

- **Total Alkalinity:** Determined by neutralization volumetry (titration) using standardized sulfuric acid (H_2SO_4 0.02 N) with mixed phenolphthalein and bromocresol green indicators, expressed in mg $CaCO_3$ L^{-1}.
- **Total Hardness, Calcium, and Magnesium:** Total Hardness was expressed as the combined concentration of calcium and magnesium in mg $CaCO_3$ L^{-1}. The calcium fraction (mg Ca^{2+} L^{-1}) was quantified via complexometric titration with EDTA at high pH (12–13) to precipitate magnesium as $Mg(OH)_2$, using murexide as a selective indicator. Magnesium (mg Mg^{2+} L^{-1}) was calculated stoichiometrically by subtracting calcium from total hardness.

- **Total Chloride:** Determined via Mahr argentometric titration using standardized silver nitrate ($AgNO_3$ 0.0141 N) and potassium chromate (K_2CrO_4) indicator. End-point precipitation of orange silver chromate indicated complete chloride consumption, expressed in mg Cl^- L^{-1}.
- **Dissolved Oxygen (DO) and Biochemical Oxygen Demand (BOD):** DO was quantified using the unmodified Winkler method (iodometry). Dissolved oxygen oxidizes manganous sulfate in an alkaline medium to form a brown manganese precipitate. Following acidification with potassium iodide and sulfuric acid, liberated elemental iodine was titrated with sodium thiosulfate. BOD was determined by measuring initial DO and remaining DO after 5 days of incubation at 20 °C in the dark, expressed in mg O_2 L^{-1}.

Nutrients and Nitrogenous/Phosphoric Forms

- **Phosphorus (Total):** Subjected to acid digestion under heat to convert polyphosphates and organic phosphorus to orthophosphate (PO_4^{3-}). Orthophosphate reacted with ammonium molybdate to form molybdophosphoric acid, which was reduced with stannous chloride to molybdenum blue and measured spectrophotometrically, expressed in mg P L^{-1}.
- **Nitrite (NO_2^-):** Determined by diazotization in an acidic medium (pH 2.0–2.5) between sample nitrite and sulfanilamide. The resulting diazo compound reacted with N-(1-naphthyl)-ethylenediamine dihydrochloride to form a reddish-purple azo dye quantified colorimetrically, expressed in mg N-NO_2^- L^{-1}.
- **Ammonia Nitrogen (NH_3 + NH_4^+):** Quantified via reaction with Nessler's reagent, forming a yellow-brown complex whose intensity is directly proportional to the sum of free ammonia and ammonium ions, expressed in mg N-NH_3 L^{-1}.
- **Total Sulfide:** Determined in acidified samples by reaction with N,N-dimethyl-p-phenylenediamine and ferric chloride ($FeCl_3$), producing a methylene blue complex measured colorimetrically, expressed in mg S^{2-} L^{-1}.
- **Sulfate (SO_4^{2-}):** Determined turbidimetrically using a commercial reagent (SulfaVer 4 / Powder Pillow). Sulfate ions react with barium chloride to form a colloidal barium sulfate ($BaSO_4$) suspension, measured turbidimetrically in mg SO_4^{2-} L^{-1}.

Dissolved and Total Metals

- **Aluminium (Total Al^{3+}):** Measured via complexation with Eriochrome Cyanine R dye in a pH 6.0 buffered solution, forming a pink-to-purple complex with an absorption peak at 535 nm, expressed in mg Al^{3+} L^{-1}.
- **Iron (Total):** Ferric iron (Fe^{3+}) was reduced to ferrous iron (Fe^{2+}) by boiling with hydrochloric acid (HCl) and hydroxylamine. Samples were then treated with 1,10-phenanthroline in a buffered medium (pH 3.2–3.3), forming an orange-red soluble chelate measured spectrophotometrically, expressed in mg Fe L^{-1}.
- **Manganese (Total):** Determined by the PAN method. Ascorbic acid reduced oxidized forms to Mn^{2+}, followed by alkaline cyanide addition to mask metallic interferences. The 1-(2-pyridylazo)-2-naphthol (PAN) indicator produced an orange complex measured spectrophotometrically, expressed in mg Mn L^{-1}.

2.3 MICROBIOLOGICAL ANALYSIS

Microbiological profiling focused on detecting and quantifying *Escherichia coli* and Total Coliforms density. The enzymatic chromogenic/fluorogenic substrate method in multi-well trays (Quanti-Tray®/Colilert) was employed based on ONPG (coliforms) and MUG (*E. coli*) cleavage. After incubation at 35 ± 0.5 °C for 24 hours, positive wells were counted and statistically converted to Most Probable Number per 100 mL (MPN 100 mL^{-1}).

2.4 WATER QUALITY INDEX (*WQI*)

Observed values for water quality parameters were evaluated against standards established by CONAMA Resolution No. 357/2005 and related regulations, such as CONAMA No. 274/2000 (CONAMA, 2000) for primary contact recreation (bathing).

For global water quality evaluation, the *WQI* originally developed by the National Sanitation Foundation (NSF-*WQI*) and adapted by the Environmental Agency of São Paulo State (CETESB, 2014) for tropical water bodies was applied. *WQI* was calculated as the weighted product of individual quality sub-indices for nine physicochemical and microbiological parameters, according to the standard weighted product equation:

$$WQI = \prod_{i=1}^{n} qi^{Wi} \qquad (1)$$

Where:

WQI: Water Quality Index, ranging on a scale from 0 to 100;

qi: sub-index or quality score of the *i*-th parameter (dimensionless value between 0 and 100), obtained from standardized rating curves;

wi: relative weight assigned to the *i*-th parameter, reflecting its relative importance in determining water quality, such that $\sum_{i=1}^{n} Wi = 1$;

n: number of parameters comprising the index (*n* = 9).

The nine parameters comprising the WQI and their respective relative weights (*wi*) are: DO = 0.17, *E. coli* = 0.15, pH = 0.12, BOD = 0.10, Ammonia Nitrogen = 0.10, Phosphorus = 0.10, Turbidity = 0.08, TDS = 0.03 (Sum ∑*wi* = 0.85).

Based on the final calculated numerical *WQI*, water quality was categorized into five classes: Very Poor (0 ≤ *WQI* ≤ 19), Poor (20 ≤ *WQI* ≤ 36), Moderate (37 ≤ *WQI* ≤ 50), Good (51 ≤ *WQI* ≤ 79), and Excellent (80 ≤ *WQI* ≤ 100).

2.5 EXPERIMENTAL DESIGN AND STATISTICAL ANALYSES

The study followed a 3 × 2 factorial experimental design, combining a spatial factor with three sampling sites (Conservation Unit, Agricultural Area, and Urban Area) and a temporal factor with two seasonal periods (Rainy Season and Dry Season). For each site-period combination, *n* = 3 independent replicates were analyzed (each replicate representing the mean of three observations), yielding *n* = 54 total observations. To reduce skewness and stabilize variance in microbiological data, counts of *E. coli* and Total Coliforms were logarithmic transformed ($\log_{10}(x)$). Residual normality was evaluated using the Shapiro-Wilk test, and variance homogeneity was checked via Levene's test. Two-way factorial ANOVA (3 × 2) was applied to evaluate the spatial, temporal, and interactive effects on individual physicochemical and microbiological parameters. For variables showing statistical significance ($p < 0.05$), Tukey's HSD post-hoc test was performed for pairwise comparisons between sites and seasons.

Overall associations among quantitative parameters were evaluated using Pearson correlation matrix, identifying the direction and magnitude of covariances ($p < 0.05$). To explore spatiotemporal variability in an integrated manner and address multicollinearity and scale differences, Hierarchical Cluster Analysis (HCA) was performed on Z-score standardized data. Distance matrices were calculated using Euclidean distance, and hierarchical linkage was generated via Ward's method (ward.D2), minimizing intra-cluster

variance. Results were visualized using dendrograms bounded by cluster partitions. All statistical routines, matrix manipulations, and graphics were rendered in R (version 4.6.1) (R Core Team, 2026), using tidyverse for data manipulation and descriptive statistics (Wickham *et al.,* 2019), factoextra for ordination (Kassambara and Mundt, 2026), and dendextend for dendrogram customization (Tal Galili, 2015).

3 RESULTS AND DISCUSSION

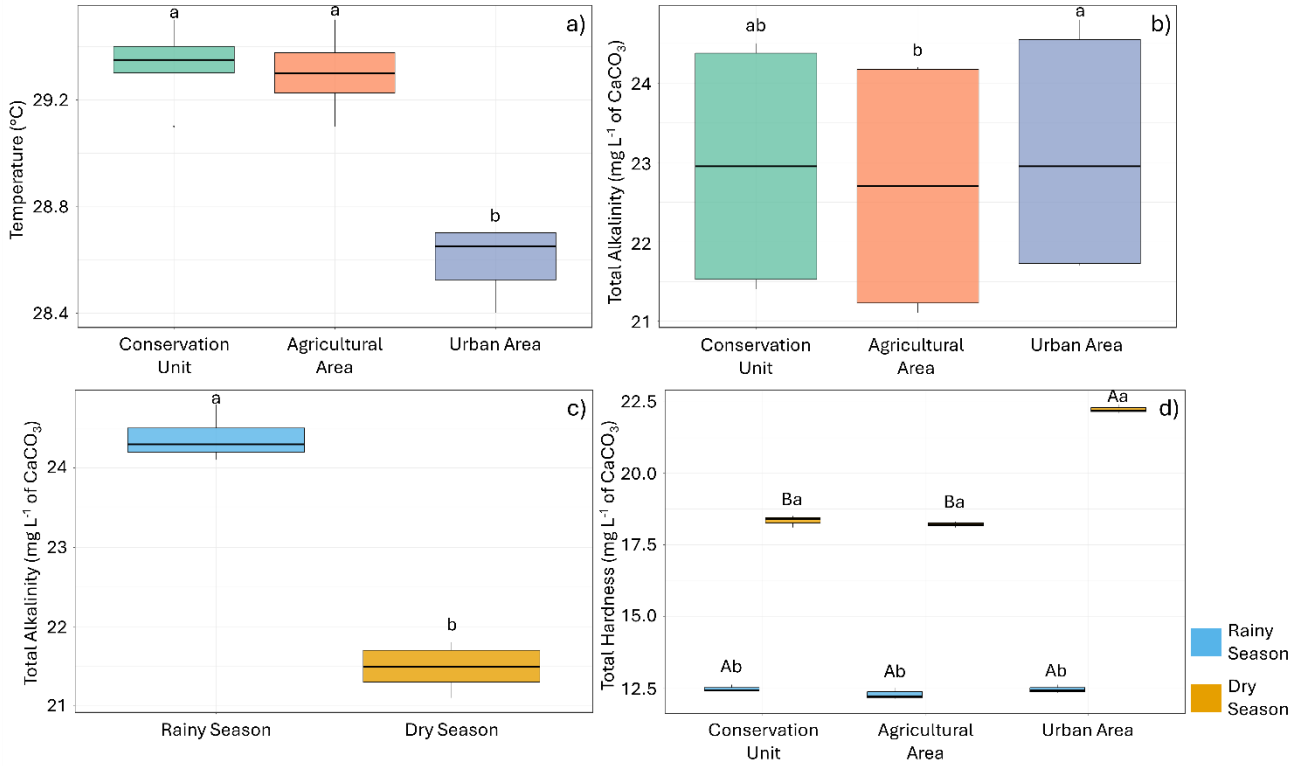
No significant differences were observed for water temperature, Fluoride, Sulfate, Sulfide, and Iron concentrations across sampling points or seasonal periods. However, ambient temperature varied significantly across evaluated areas ($p < 0.05$). The highest ambient temperatures were recorded in the Conservation Unit (29.33 °C) and Agricultural Area (29.30 °C), which did not differ significantly from each other ($p = 0.889$) (Figure 3a). Conversely, the Urban Area exhibited significantly lower ambient temperature values (28.60 °C).

Total Alkalinity ranged from 21.1 to 24.8 mg L^{-1} of $CaCO_3$ across sampling sites (Figure 3b). The Urban Area recorded the highest mean values (23.13 mg L^{-1} of $CaCO_3$), showing a statistically significant difference compared to the Agricultural Area (22.68 mg L^{-1} of $CaCO_3$, $p = 0.001$). The Conservation Unit exhibited intermediate values (22.95 mg L^{-1} of $CaCO_3$, $p = 0.200$), differing non-significantly from either urban or agricultural areas. Total Alkalinity was also significantly affected by season ($p < 0.05$) (Figure 3c), with the Rainy Season exhibiting higher levels (24.33 mg L^{-1} of $CaCO_3$) than the Dry Season (21.47 mg L^{-1} of $CaCO_3$).

Total Hardness demonstrated seasonal and spatial variations, as well as a significant interaction between these factors ($p < 0.05$). Across all areas, Total Hardness was significantly higher during the Dry Season compared to the Rainy Season ($p < 0.05$). In the Rainy Season, hardness remained low and uniform (mean of 12.38 mg L^{-1} of $CaCO_3$) across all land uses (Figure 3d). During the Dry Season, the Urban Area exhibited the highest Total Hardness (22.23 mg L^{-1} of $CaCO_3$), being significantly higher than the Conservation Unit ($p < 0.05$) and Agricultural Area ($p < 0.05$), which maintained values of 18.33 and 18.20 mg L^{-1} of $CaCO_3$, respectively, without differing from each other ($p = 0.905$).

Figure 3

Water physicochemical parameters: a – Temperature; b – Total Alkalinity by land use; c – Total Alkalinity by season; and d – Total Hardness observed in the Campo Alegre Stream Basin, GO, Brazil, across land uses (Conservation Unit, Agricultural Area, Urban Area) and seasonal periods (Rainy Season, Dry Season). Distinct letters indicate statistically significant differences ($p < 0.05$, Tukey test). In Figure 3d, uppercase letters compare seasonal periods within the same land use, whereas lowercase letters compare land uses within the same season. Boxplots represent the median, quartiles (25% and 75%), and min/max values.



DO, BOD, Ammonia Nitrogen, and Nitrate displayed significant variations driven by the interaction between land use and seasonal period ($p < 0.05$; Figure 4). During the Rainy Season, DO concentrations peaked in the Conservation Unit and Urban Area (7.53 and 7.66 mg L^{-1} of O_2, respectively, $p = 0.664$), being significantly higher than in the Agricultural Area ($p < 0.05$) (Figure 4a). In the Dry Season, a generalized reduction in DO occurred, with the highest value in the Agricultural Area (7.43 mg L^{-1} of O_2), followed by the Urban Area (7.03 mg L^{-1} of O_2) and Conservation Unit (6.63 mg L^{-1} of O_2), all significantly different from one another ($p < 0.05$). Only in the Agricultural Area were DO levels higher in the dry period than in the rainy period.

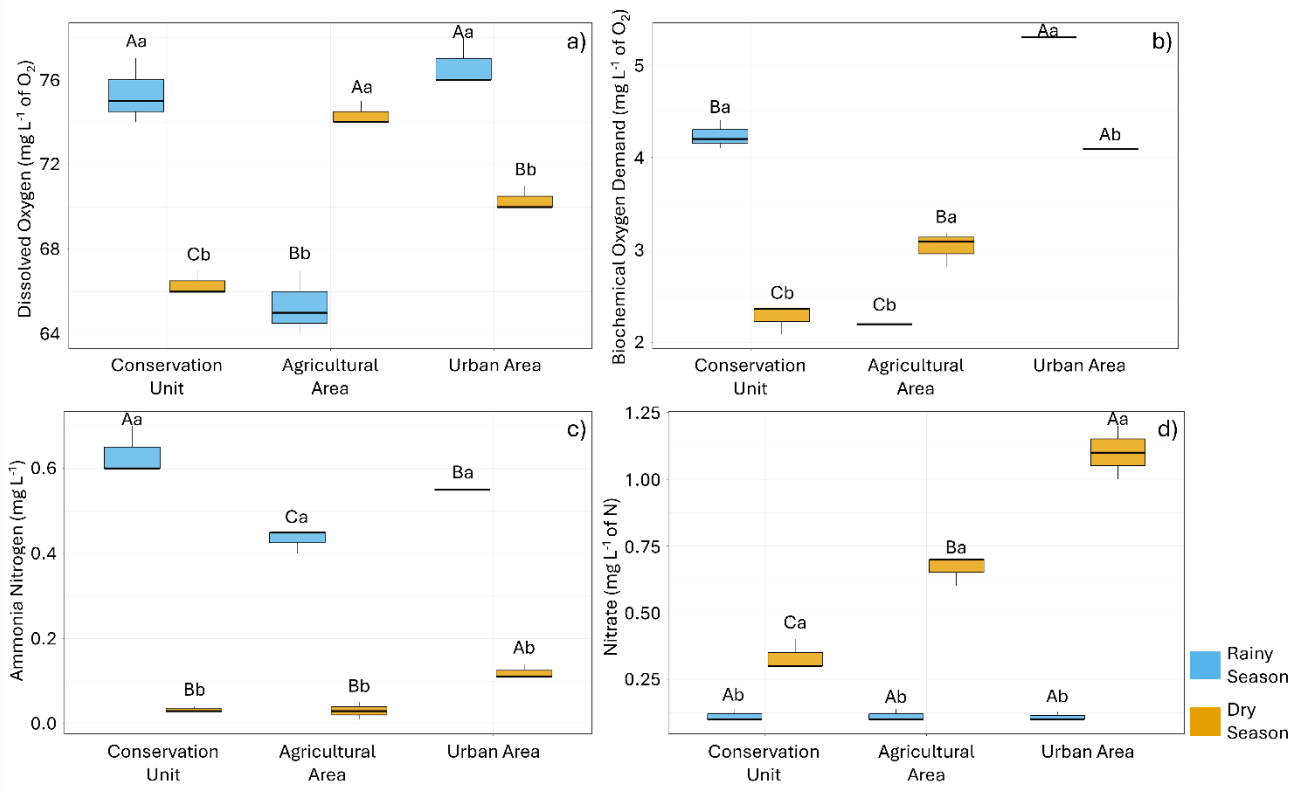
BOD peaked in the Urban Area during the Rainy Season (5.30 mg L^{-1} of O_2). In the same season, the Conservation Unit showed intermediate values (4.23 mg L^{-1} of O_2), whereas the Agricultural Area recorded the lowest concentrations (2.20 mg L^{-1} of O_2) (Figure 4b). In the Dry Season, a partial reversal occurred in rural/natural zones: the Agricultural Area showed higher BOD than in the Rainy Season (3.03 mg L^{-1} of O_2), whereas the Conservation Unit showed reduced values (2.27 mg L^{-1} of O_2). The Urban Area sustained the highest BOD in the Dry Season as well (4.09 mg L^{-1} of O_2), though statistically lower than its own peak in the Rainy Season.

Ammonia Nitrogen concentrations exhibited a strong seasonal pattern ($p < 0.05$) (Figure 4c). In the Rainy Season, the highest levels were recorded across all areas, peaking in the Conservation Unit (0.66 mg L^{-1}), followed by the Urban Area (0.55 mg L^{-1}) and Agricultural Area (0.43 mg L^{-1}), with significant differences among all three ($p < 0.05$). In the Dry Season, Ammonia Nitrogen dropped near zero in the Conservation Unit and Agricultural Area (0.033 and 0.030 mg L^{-1}, respectively, $p = 0.999$), remaining slightly higher in the Urban Area (0.12 mg L^{-1}).

Nitrate exhibited an opposite seasonal trend compared to Ammonia Nitrogen. During the Rainy Season, Nitrate values remained low and baseline across all land uses (Figure 4d). In the Dry Season, Nitrate concentrations increased significantly across all land uses, with an exponentially higher increase in the Urban Area (1.10 mg L^{-1} of N), followed by the Agricultural Area (0.66 mg L^{-1} of N) and Conservation Unit (0.33 mg L^{-1} of N).

Figure 4

Oxygenation indicators and nutrients in water: a – DO; b – BOD; c – Ammonia Nitrogen; and d – Nitrate observed in the Campo Alegre Stream Basin, GO, Brazil, across land uses and seasonal periods. Uppercase letters compare seasons within the same land use; lowercase letters compare land uses within the same season ($p < 0.05$, Tukey test). Boxplots represent the median, quartiles, and min/max values.



Nitrite, Phosphorus, Calcium, and Magnesium exhibited significant variations according to land use and season ($p < 0.05$). Nitrite concentration peaked in the Urban Area during the Rainy Season (0.11 mg L^{-1} of N), significantly exceeding ($p < 0.05$) all other areas and the dry period (Figure 5a). In the conservation and agricultural areas, Nitrite concentrations remained near zero across both seasons.

Conversely, the highest Phosphorus concentrations occurred during the Dry Season (Figure 5b). The Urban Area recorded the highest Phosphorus levels in the Dry Season (0.03 mg L^{-1} of P), followed by the Conservation Unit (0.01 mg L^{-1} of P) and Agricultural Area (0.005 mg L^{-1} of P), with significant differences among all three ($p < 0.05$). During the Rainy Season, Phosphorus remained at extremely low or undetectable levels in all areas.

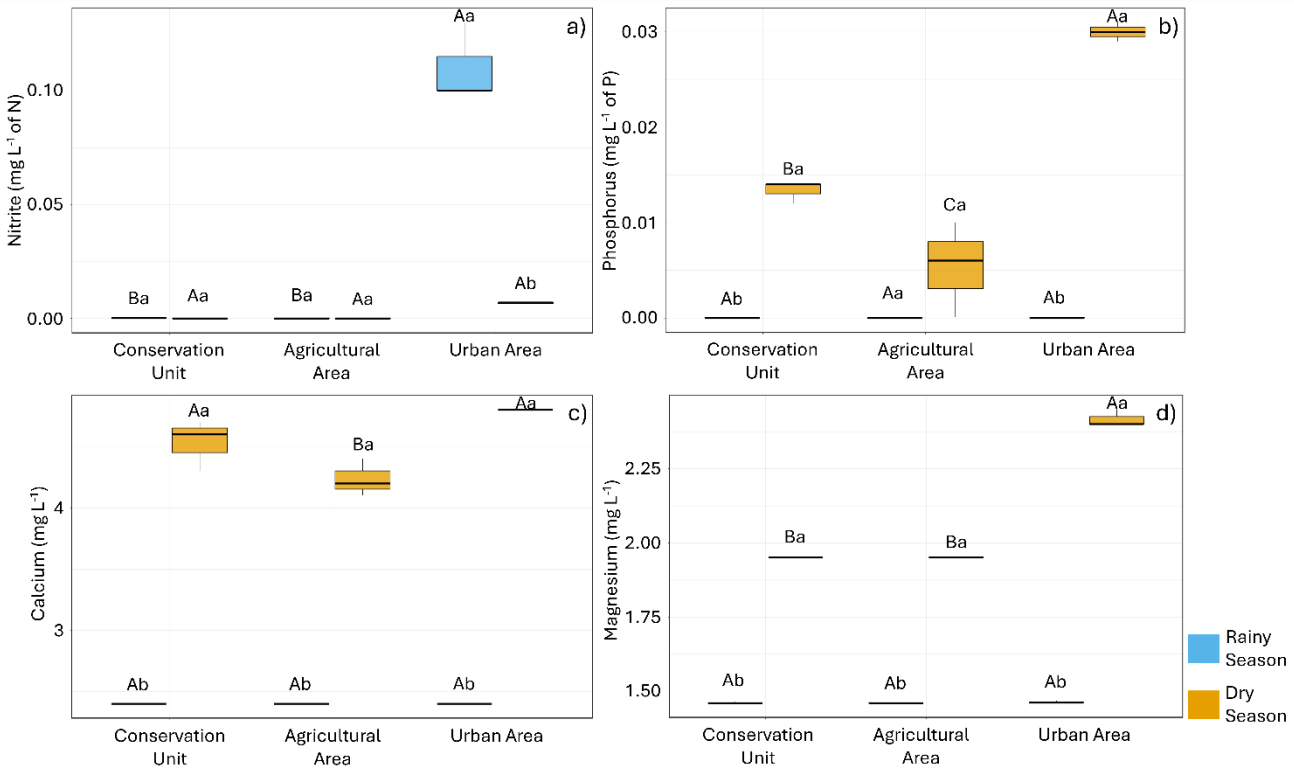
Calcium and Magnesium concentrations demonstrated a marked seasonal pattern, with substantially higher values in the Dry Season compared to the Rainy Season across all

evaluated environments ($p < 0.05$) (Figures 5c and 5d). During the Dry Season, highest Calcium concentrations occurred in the Urban Area (4.80 mg L^{-1}), followed by the Conservation Unit (4.53 mg L^{-1}) and Agricultural Area (4.23 mg L^{-1}) (Figure 5c). In the Rainy Season, Calcium levels dropped uniformly to approximately 2.40 mg L^{-1} across all areas.

During the Dry Season, Magnesium concentrations were significantly higher in the Urban Area (2.41 mg L^{-1}) compared to the Agricultural Area (1.95 mg L^{-1}) and Conservation Unit (1.95 mg L^{-1}) (Figure 5d). In the Rainy Season, Magnesium fell to ~1.46 mg L^{-1} without significant variation among land uses.

Figure 5

Nutrients in water: a – Nitrite; b – Phosphorus; c – Calcium; and d – Magnesium observed in the Campo Alegre Stream Basin, GO, Brazil, across land uses and seasonal periods. Uppercase letters compare seasons within the same land use; lowercase letters compare land uses within the same season ($p < 0.05$, Tukey test). Boxplots represent median, quartiles, and min/max values.



Chloride, Manganese, Aluminium, and TDS demonstrated statistically significant variations in response to land use and season ($p < 0.05$) (Figure 6). Highest Chloride concentrations occurred in the Rainy Season across all land uses, peaking in the Agricultural

Area (1.43 mg L^{-1} of Cl^-), followed by the Conservation Unit (1.30 mg L^{-1} of Cl^-) and Urban Area (1.16 mg L^{-1} of Cl^-) (Figure 6a). In the Dry Season, Chloride dropped near zero in the Conservation Unit and Agricultural Area (p = 0.472). However, in the Urban Area, Chloride levels remained elevated during the Dry Season (1.10 mg L^{-1} of Cl^-), displaying no significant difference from its rainy season levels (p = 0.932).

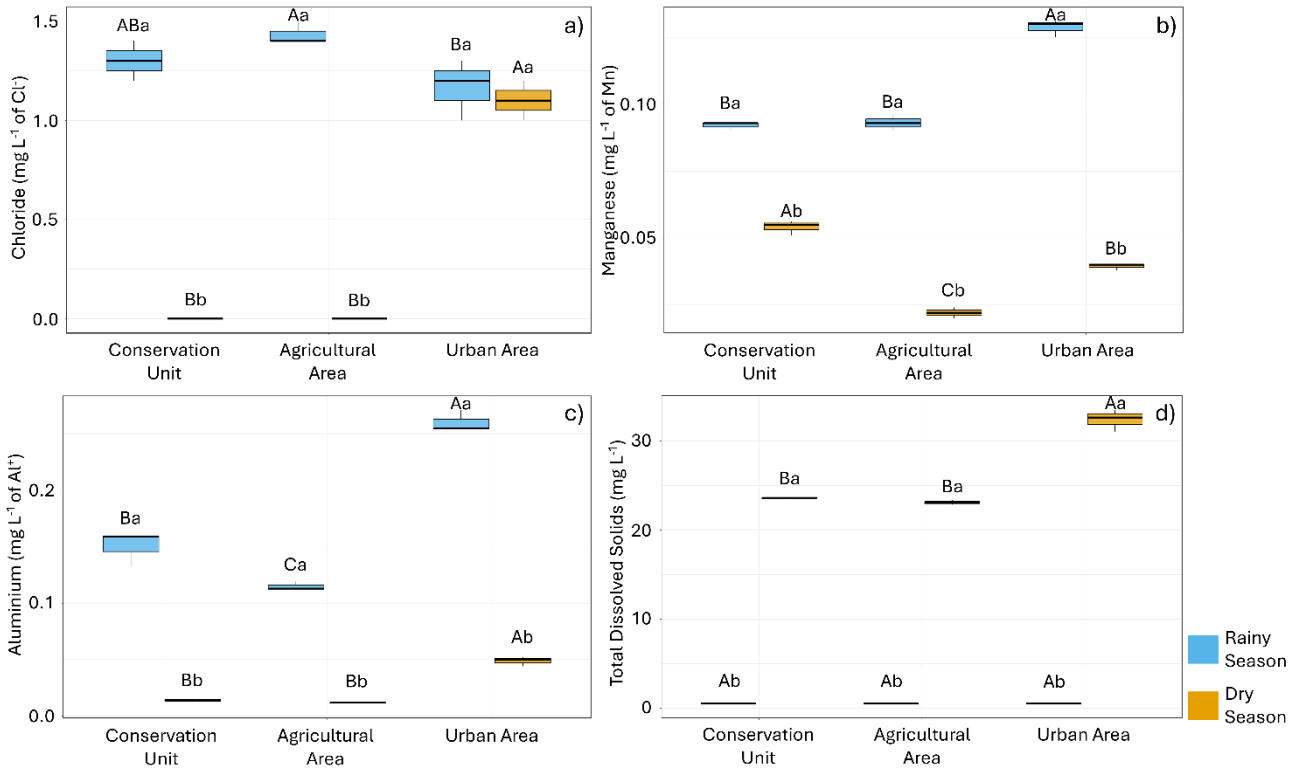
In the Rainy Season, Manganese peaked in the Urban Area (0.12 mg L^{-1} of Mn), while the Conservation Unit and Agricultural Area recorded identical, significantly lower values (0.09 mg L^{-1} of Mn) (Figure 6b). In the Dry Season, Manganese levels dropped significantly across all areas ($p < 0.05$), with the highest remaining value in the Conservation Unit (0.05 mg L^{-1} of Mn), followed by the Urban Area (0.03 mg L^{-1} of Mn) and Agricultural Area (0.02 mg L^{-1} of Mn).

Aluminium concentrations were markedly higher in the Rainy Season across all areas ($p < 0.05$), peaking in the Urban Area (0.26 mg L^{-1} of Al^{3+}), followed by the Conservation Unit (0.15 mg L^{-1} of Al^{3+}) and Agricultural Area (0.11 mg L^{-1} of Al^{3+}) (Figure 6c). In the Dry Season, concentrations remained very low in the Conservation Unit and Agricultural Area, while the Urban Area sustained significantly higher levels (0.04 mg L^{-1} of Al^{3+}, $p < 0.05$).

TDS displayed an inverse seasonal trend relative to metals and chloride, with substantially higher concentrations in the Dry Season compared to the Rainy Season across all land uses ($p < 0.05$) (Figure 6d). During the Dry Season, the Urban Area exhibited the highest TDS value (32.35 mg L^{-1}), significantly higher than the Agricultural Area and Conservation Unit (23.08 and 23.56 mg L^{-1}, respectively, p = 0.857). In the Rainy Season, TDS levels fell near zero across all areas.

Figure 6

Nutrients and Total Dissolved Solids in water: a – Chloride; b – Manganese; c – Aluminium; and d – TDS observed in the Campo Alegre Stream Basin, GO, Brazil, across land uses and seasonal periods. Uppercase letters compare seasons within the same land use; lowercase letters compare land uses within the same season ($p < 0.05$, Tukey test). Boxplots represent median, quartiles, and min/max values.



EC, pH, Apparent Color, and Turbidity also exhibited significant variations depending on land-use class and season (Figure 7). EC revealed an evident seasonal pattern, with substantially higher values in the Dry Season compared to the Rainy Season across all land uses ($p < 0.05$) (Figure 7a). During the Dry Season, the Urban Area recorded the maximum value (58.83 µS cm^{-1}), significantly exceeding the Agricultural Area and Conservation Unit (41.96 and 42.83 µS cm^{-1}, respectively, $p = 0.992$). In the Rainy Season, the Urban Area also exhibited the highest conductivity (34.60 µS cm^{-1}), while the Conservation Unit and Agricultural Area showed lower values (30.66 and 29.96 µS cm^{-1}, respectively, $p = 0.997$).

pH values were significantly higher in the Dry Season than in the Rainy Season across all areas ($p < 0.05$) (Figure 7b). In the Dry Season, highest pH values were observed in the Agricultural Area and Urban Area (7.09 and 7.06, respectively, $p = 0.966$), exceeding the Conservation Unit (6.84). In the Rainy Season, the Agricultural Area maintained near-neutral

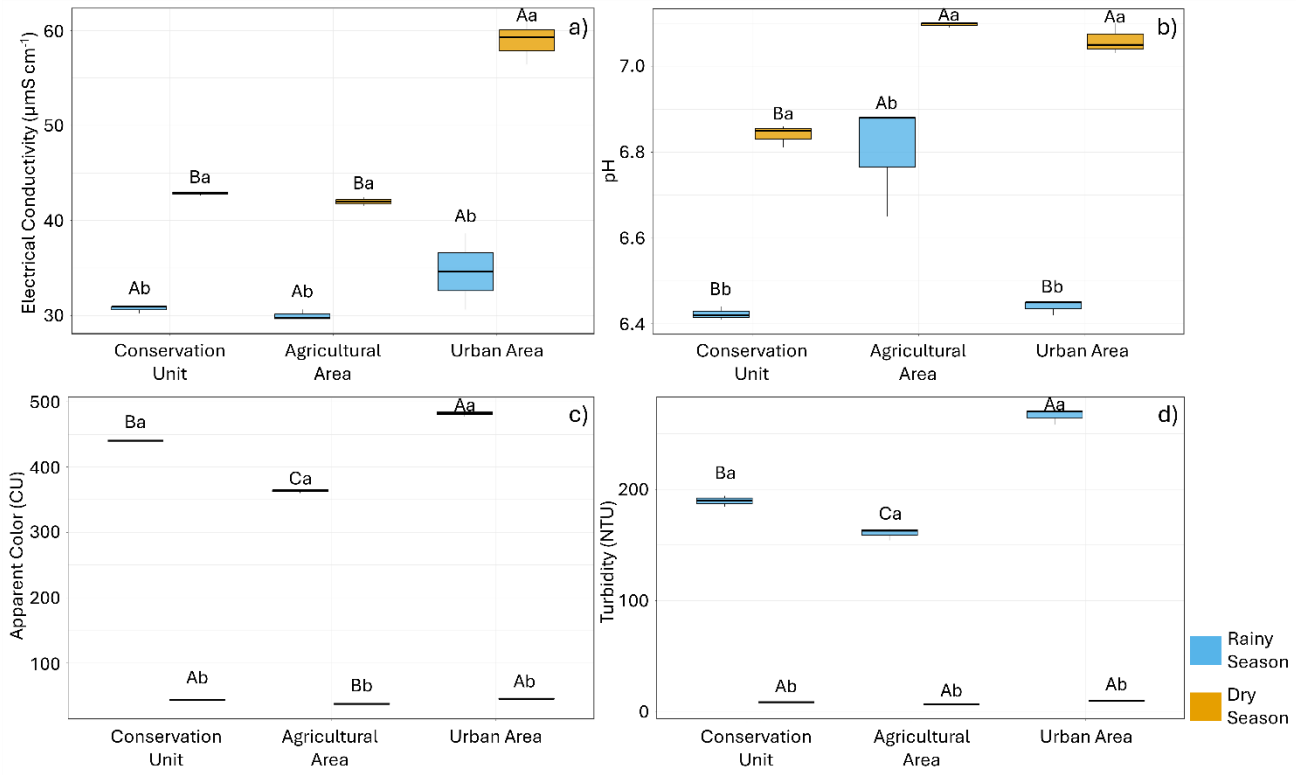
pH (6.80), significantly higher than the Conservation Unit and Urban Area, which exhibited more acidic values (6.42 and 6.44, respectively, $p = 0.999$).

Apparent Color and Turbidity exhibited inverse seasonal dynamics compared to EC and pH, with marked increases during the Rainy Season across all sampling sites ($p < 0.05$) (Figures 7c and 7d). During the Rainy Season, the Urban Area recorded the highest Apparent Color (481.66 CU), followed by the Conservation Unit (440.33 CU) and Agricultural Area (366.33 CU), showing significant differences among all three land uses ($p < 0.05$) (Figure 7c). In the dry season, Apparent Color dropped sharply below 45 CU at all sites.

In the Rainy Season, Turbidity was significantly higher in the Urban Area (266.00 NTU), followed by the Conservation Unit (189.33 NTU) and Agricultural Area (160.33 NTU) ($p < 0.05$) (Figure 7d). In the Dry Season, Turbidity fell to residual levels below 11.15 NTU across all evaluated areas.

Figure 7

Physicochemical parameters in water: a – Electrical Conductivity; b – pH; c – Apparent Color; and d – Turbidity observed in the Campo Alegre Stream Basin, GO, Brazil, across land uses and seasonal periods. Uppercase letters compare seasons within the same land use; lowercase letters compare land uses within the same season (p < 0.05, Tukey test). Boxplots represent median, quartiles, and min/max values.

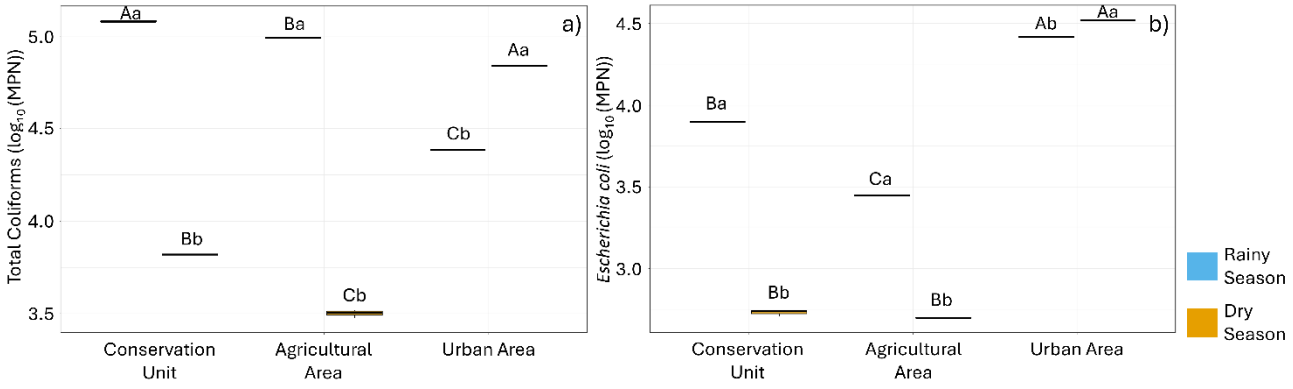


Total Coliforms and *E. coli* concentrations exhibited significant variations driven by land use and seasonality (Figure 8). Overall, the Rainy Season promoted a statistically significant increase in both microbiological indicators across all evaluated areas ($p < 0.05$). For Total Coliforms (Figure 8a), highest Rainy Season values occurred in the Conservation Unit and Agricultural Area (5.08 and 4.99 $\log_{10}$ [MPN], respectively; $p < 0.05$), exceeding the Urban Area. In the Dry Season, the Urban Area maintained the highest Total Coliform levels (4.83 $\log_{10}$ [MPN]), whereas the Agricultural Area exhibited the lowest observed value (3.50 $\log_{10}$ [MPN]).

Regarding *E. coli* (Figure 8b), the Urban Area stood out with the highest concentrations in both seasons (4.41 $\log_{10}$ [MPN] in the Rainy Season and 4.51 $\log_{10}$ [MPN] in the Dry Season, $p < 0.05$). During the Rainy Season, contamination decreased progressively from the Urban Area to the Conservation Unit (3.89 $\log_{10}$ [MPN]) and Agricultural Area (3.44 $\log_{10}$ [MPN]). In the Dry Season, the Conservation Unit and Agricultural Area showed drastic reductions in *E. coli* levels, reaching similar baseline values (2.70 $\log_{10}$ [MPN], $p < 0.05$).

Figure 8

Microbiological parameters in water: a – Total Coliforms; and b – Escherichia coli observed in the Campo Alegre Stream Basin, GO, Brazil, across land uses and seasonal periods. Uppercase letters compare seasons within the same land use; lowercase letters compare land uses within the same season ($p < 0.05$, Tukey test). Boxplots represent median, quartiles, and min/max values.



Pearson correlation analysis revealed significant associations among analyzed physicochemical and microbiological parameters (Figure 9). A strong positive cluster was observed among Apparent Color, Turbidity, and Aluminium ($r = 0.98$), which also displayed high correlations with Total Alkalinity ($r = 0.94$) and Manganese ($r = 0.88$). This behavior

suggests a common source driving particulate matter and metal transport into the aquatic matrix.

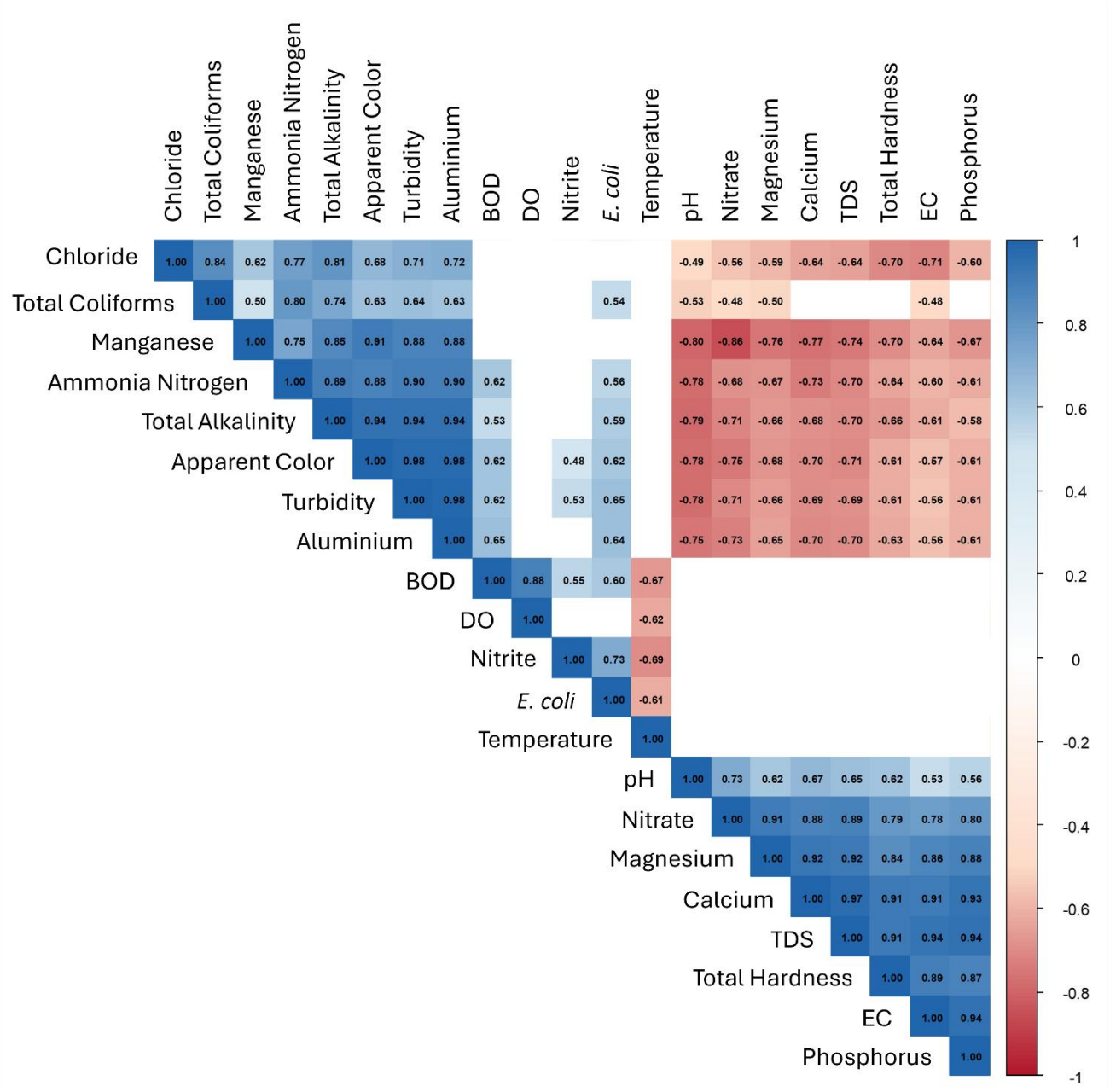
Parameters related to mineralization and dissolved solids (pH, Nitrate, Magnesium, Calcium, TDS, Total Hardness, EC, and Phosphorus) formed a second strongly interrelated cluster ($r > 0.78$ for most pairs). Notable associations included Calcium and TDS (r = 0.97), as well as EC, TDS, and Phosphorus ($r = 0.94$). Interestingly, this solids-and-minerals group showed moderate to strong negative correlations with the turbidity, color, and metals group (e.g., Manganese vs. Nitrate, $r = -0.86$; Total Alkalinity vs. pH, $r = -0.79$).

Microbiological indicators correlated directly with organic matter and effluent parameters. Total Coliforms density correlated positively with Chloride ($r = 0.84$), Ammonia Nitrogen ($r = 0.77$), and Total Alkalinity ($r = 0.74$). In turn, *E. coli* exhibited significant positive correlations with Nitrite ($r = 0.73$), Turbidity ($r = 0.65$), Aluminium ($r = 0.64$), Apparent Color ($r = 0.62$), and BOD ($r = 0.60$), alongside a moderate association with Total Coliforms ($r = 0.54$).

Ambient temperature showed an inverse relationship with organic contamination and microbiological parameters, correlating negatively with Nitrite ($r = -0.69$), BOD ($r = -0.67$), DO ($r = -0.62$), and *E. coli* ($r = -0.61$).

Figure 9

Pearson correlation matrix among water quality parameters in the Campo Alegre Stream Basin, GO, Brazil. Correlation coefficients (r) range from -1.0 (strong negative, red) to +1.0 (strong positive, blue). Blank cells indicate non-significant correlations (p > 0.05). BOD: Biochemical Oxygen Demand; DO: Dissolved Oxygen; TDS: Total Dissolved Solids; EC: Electrical Conductivity.



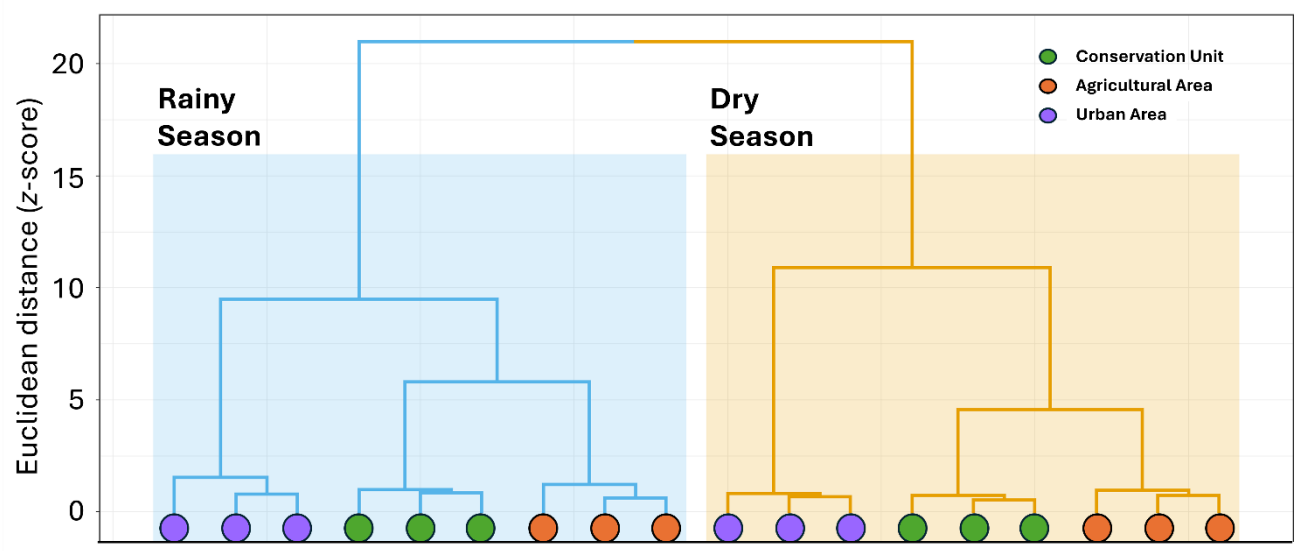
HCA applied to Z-score normalized data revealed a clear sample separation governed primarily by seasonality and secondarily by land use (Figure 10). At an Euclidean distance greater than 21.70, the dendrogram split into two strictly defined main clusters: the first

containing all Rainy Season samples and the second grouping all Dry Season samples. This demonstrates that dynamic changes associated with rainfall regime exert the largest magnitude impact on water physicochemical and microbiological characteristics.

Furthermore, within each seasonal cluster, a perfect sub-clustering into three subgroups occurred (Euclidean distance of 9.75), strictly matching the three studied land uses: Conservation Unit, Agricultural Area, and Urban Area. The small intra-group distance among local replicates (< 2) reflects high consistency and reproducibility among monitored parameters within each site.

Figure 10

Hierarchical Cluster Analysis (HCA) dendrogram based on Euclidean distance (Z-score standardized data) for water samples from the Campo Alegre Stream Basin, GO, Brazil, across land uses (Conservation Unit, Agricultural Area, Urban Area) and seasonal periods (Rainy Season, Dry Season).



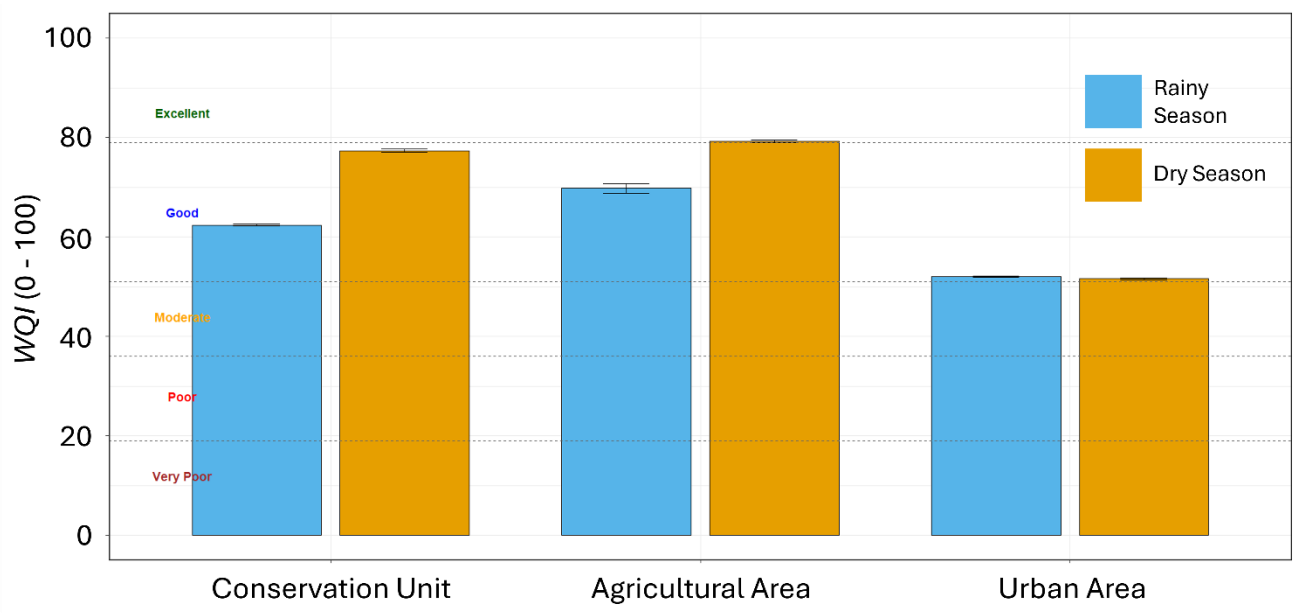
Water Quality Index (*WQI*) values varied as a function of land use and seasonality (Figure 11). The Urban Area presented the lowest overall *WQI* values, remaining stabilized at ~52 in both the Rainy Season and Dry Season, placing its water quality at the lower boundary of the Good category, near the Moderate threshold. The absence of seasonal *WQI* variation in the Urban Area reflects continuous anthropogenic pollutant loads throughout the year.

Conversely, the Conservation Unit and Agricultural Area exhibited marked seasonal sensitivity, recording significant water quality improvement during the Dry Season (Figure 11).

In the Conservation Unit, *WQI* rose from 62.5 in the Rainy Season to 77.2 in the Dry Season, remaining within the Good classification. The Agricultural Area achieved the highest quality scores, ranging from 69.8 in the Rainy Season (Good) to 79.2 in the Dry Season, reaching the Excellent tier. The Rainy Season *WQI* drop in these two sites is attributable to surface runoff carrying sediments, nutrients, and organic matter.

Figure 11

Water Quality Index (WQI, scale 0 to 100) for water samples observed in the Campo Alegre Stream Basin, GO, Brazil, across land uses (Conservation Unit, Agricultural Area, Urban Area) and seasonal periods (Rainy Season, Dry Season). Horizontal dashed lines mark quality boundaries: Very Poor, Poor, Moderate, Good, and Excellent. Error bars represent standard deviations.



3.1 SEASONALITY ACTED AS A DOMINANT HYDROLOGICAL FORCE, ELEVATING WATER TURBIDITY, ALUMINIUM, AND MANGANESE CONCENTRATIONS DURING THE RAINY SEASON

According to CONAMA Resolution No. 357/2005, Class 2 waters are designated for human supply following conventional treatment, aquatic community protection, primary recreation, irrigation, aquaculture, and fishing. For these uses, Turbidity must not exceed 100 NTU. In the Dry Season, values observed in the Campo Alegre Basin remained well below this threshold. However, during the Rainy Season, sampling areas severely violated the legal threshold, particularly in the urban stretch. This confirms that sediment runoff during rain

events compromises raw water quality for drinking water treatment (Alkhadher *et al.,* 2025; Li *et al.,* 2024; Delpla *et al.,* 2023). Beyond treatment complications, excessive suspended solids directly degrade aquatic biota by attenuating solar radiation and inhibiting phytoplankton photosynthesis, thereby reducing primary production (Birmachu *et al.,* 2024). Suspended matter also induces mechanical abrasion and respiratory stress on fish and invertebrate gills, reduces visibility for visual predators (Zanghi and Ioannou, 2025; Lowe *et al.,* 2015), and upon settling, silts the riverbed, destroying benthic habitats and spawning sites (Sahoo and Anandhi, 2023), while serving as a vector for metal and nutrient transport (Nasrabadi *et al.,* 2016; Bladon *et al.,* 2014).

The concentration of Aluminium (Al^{3+}) in Class 2 waters must not exceed 0.1 mg L^{-1}. Thus, during the Rainy Season, sampling sites - especially the Urban Area - exceeded chronic toxicity limits, suggesting strong influence from the leaching of enriched clay soils (Gunes, 2022) (typical of the Cerrado) and urban effluent contamination (Pochodyła-Ducka *et al.,* 2023). High Aluminium concentrations exert severe ecotoxic effects on aquatic biota, acting as a major biological stressor in freshwater ecosystems (Botté *et al.,* 2022). In fish, free Al^{3+} binds to gill epithelia, inducing mucus hypersecretion, histological lesions, ionoregulatory dysfunction, and severe hypoxia due to impaired gas exchange, potentially leading to asphyxiation and mass mortality (Hadi and Alwan, 2012; Exley *et al.,* 1991). In benthic invertebrates and phytoplankton, elevated aluminium alters cell membrane permeability, inhibits essential metabolic enzymes, and induces oxidative stress, resulting in reduced survival rates, impaired growth, and local biodiversity decline (Schaly and Braguini, 2024; Zhang *et al.,* 2023; Nowicka, 2022). Furthermore, by affecting primary productivity and sensitive organisms at the base of the food web, excess aluminium destabilizes ecosystem population dynamics and compromises nutrient cycling and ecological integrity (Li *et al.,* 2026; Rybak *et al.,* 2026).

During the Rainy Season, Manganese concentration in the Urban Area exceeded the maximum threshold of 0.1 mg L^{-1} established by CONAMA Resolution No. 357/2005. High Total Manganese levels frequently signal anthropogenic contamination (Zhai *et al.,* 2021). In aquatic environments, manganese operates under redox dynamics: in its reduced, soluble form (Mn^{2+}), exposure to oxidizing conditions causes precipitation as manganese dioxide (Mn^{4+}), imparting a dark brown color and turbid appearance to water (Apolinário *et al.,* 2018). This physicochemical alteration and Mn accumulation severely impact aquatic life. Manganese oxyhydroxide precipitation on substrates silts the riverbed, destroying benthic

microhabitats, smothering eggs, and reducing shelter for bioindicator organisms (Wilson *et al.,* 2019). Additionally, high free Mn levels induce oxidative stress, tissue bioaccumulation, and chronic toxicity in fish and macrophytes, while biofouling and clogging gill structures in aquatic fauna (Gnocchi *et al.,* 2024; Niemiec and Wiśniowska-Kielian, 2015; Gabriel *et al.,* 2013), thereby impairing trophic dynamics in the aquatic ecosystem (Paiva *et al.,* 2025).

3.2 ANTHROPOGENIC PRESSURE IN THE URBAN AREA IMPAIRED WATER SANITARY QUALITY AND BOD DURING THE RAINY SEASON

CONAMA Resolution No. 357/2005 establishes a maximum limit of 1,000 MPN/100 mL (≈ 3.0 $\log_{10}$ [MPN]) of thermotolerant coliforms or *E. coli* for systematic sampling, or a bathing limit (CONAMA, 2000) of 800 MPN/100 mL (≈ 2.9 $\log_{10}$ [MPN]). The Urban Area remained in continuous critical non-compliance across both seasons, whereas preserved and agricultural areas returned to legal compliance in the Dry Season. Thus, chronic urban contamination confirms the persistent discharge of raw domestic sewage without seasonal mitigation.

High concentrations of thermotolerant coliforms and *E. coli* represent a critical public health and ecosystem risk (Mishra *et al.,* 2018; Poma *et al.,* 2016). For human health, these bioindicators point to direct fecal contamination from humans or animals and the circulation of enteric pathogens (such as viruses, bacteria, and protozoa), which can trigger waterborne disease outbreaks through drinking, irrigation of raw vegetables, or primary contact recreation (Soares *et al.,* 2025; WHO, 2021). From an aquatic community perspective, although *E. coli* itself is not directly toxic to fish and invertebrates, the accompanying sewage load drives metabolic activity in heterotrophic decomposers (Narayanan, 2025; Bhat and Qayoom, 2021). This process induces high BOD, depleting DO concentrations and causing potential hypoxia, anoxia, mortality of sensitive organisms, and food web collapse (Wen *et al.,* 2017; Shiddamallayya and Pratima, 2008).

Accordingly, a positive correlation was observed among *E. coli*, Turbidity, Apparent Color, and BOD. CONAMA Resolution No. 357/2005 sets a maximum BOD limit of 5.0 mg L^{-1} of O_2, while DO must not fall below this threshold. In the Rainy Season, the Urban Area reached BOD levels exceeding regulatory limits, reflecting combined sewer overflows and urban surface runoff wash. Nevertheless, all sampling points and seasons maintained high DO levels, demonstrating that despite organic inputs, the stream retains sufficient reaeration/self-purification capacity to prevent anoxia (Gao *et al.,* 2024).

3.3 SEASONALITY AFFECTED NITROGEN AND PHOSPHORUS DYNAMICS, THOUGH WITHOUT IMMINENT EUTROPHICATION RISK

The maximum Nitrite limit set by CONAMA Resolution No. 357/2005 for Class 2 freshwaters is 1.0 mg L^{-1} of N. Although the peak observed in the Urban Area during the Rainy Season remained within legal limits, this temporary rise serves as an early indicator of incomplete organic matter oxidation from raw sewage inputs (Rantanen, 2020). Because nitrite is an unstable intermediate in the nitrogen cycle - formed during the first stage of nitrification ($NH_4^+ \rightarrow NO_2^-$) or via partial denitrification (Ward *et al.,* 2011) - its detection in the water column signals a temporal bottleneck in biological oxidation rates (Aktan *et al.,* 2025). The rapid conversion of NO_2^- to NO_3^- by nitrite-oxidizing bacteria depends heavily on dissolved oxygen, aeration, and hydraulic retention time (Bolsan *et al.,* 2024). Thus, Nitrite presence in the Rainy Season reflects continuous untreated domestic effluent discharge and nitrate-reducing bacterial activity in anoxic microenvironments created by high suspended sediment loads (Zhang *et al.,* 2026).

Regarding Nitrate, CONAMA Resolution No. 357/2005 sets a Class 2 threshold of 10.0 mg L^{-1} of N. Although an exponential increase occurred during the Dry Season in the Urban Area, all values remained well within legal limits, indicating that biological conversion of ammonia to nitrate did not reach toxic thresholds for aquatic life or public health. This Dry Season Nitrate rise, alongside a sharp drop in Ammonia Nitrogen, confirms the re-establishment of complete and efficient biological nitrification ($NH_4^+ \rightarrow NO_2^- \rightarrow NO_3^-$) in the water column, favored by longer hydraulic retention time, elevated temperatures, and adequate oxygenation (Sinha and Annachhatre, 2007).

Regarding eutrophication, although Dry Season Nitrate increases nutrient availability in the Urban Area, ecosystem response is constrained by Phosphorus availability (Dodds and Smith, 2016; Lürling and van Oosterhout, 2013). Total Phosphorus concentrations remained comfortably within regulatory limits across all sites and seasons (CONAMA 357 Class 2 limit for lotic environments = 0.1 mg L^{-1} of P). Maintaining low Phosphorus levels indicates that this nutrient acts as the primary limiting factor in the system, mitigating immediate risks of severe eutrophication and cyanobacterial or macrophyte blooms (Mishra, 2023; Ibrahim *et al.,* 2022), despite greater water clarity and Nitrate availability in the dry period.

3.4 ANTHROPOGENIC PRESSURE IN THE URBAN AREA REDUCED WATER PH AND DROVE A DISTINCT PATTERN OF DEGRADATION

CONAMA Resolution No. 357/2005 requires Class 2 waters to maintain pH within 6.0–9.0. While all samples complied with this range, the slightly acidic pH observed in the Conservation Unit and Urban Area during the Rainy Season warrants ecotoxicological attention. Even within legal bounds, moderate acidification driven by rainfall enriched with atmospheric CO_2 and organic acids from decomposition alters the chemical balance of the stream (Enerijiofi *et al.,* 2026). Lower pH increases the solubility and bioavailability of heavy metals and trace elements such as free Aluminium (Al^{3+}) and Manganese (Mn^{2+}) (Aggarwal *et al.,* 2025), intensifying their bioaccumulation and toxic potential in aquatic biota (Fortin, 2024; Gerhardt, 1993; Wren and Stephenson, 1991). Additionally, minor pH drops can induce osmoregulatory stress in microcrustaceans and juvenile fish, while compromising shell and exoskeleton integrity in benthic communities, directly impacting ecosystem structure and diversity (Pourmozaffar *et al.,* 2025; Byrne and Fitzer, 2019).

HCA confirmed the unique environmental profile of the Urban Area, which segregated as an isolated spatial cluster relative to the Conservation Unit and Agricultural Area. This differentiation stems from chronic anthropogenic pressures, characterized by point-source raw sewage discharges and nonpoint urban runoff wash from impervious surfaces (Khatri and Tyagi, 2015; Taebi and Droste, 2004), overriding natural dilution and hydrological variability. This discrepancy was directly reflected in WQI scores: while preserved and agricultural areas maintained Good-to-Excellent ratings with clear Dry Season recovery, the urban stretch displayed persistent degradation, hovering near the Moderate threshold year-round. Urban WQI was heavily penalized by persistent non-compliance in *E. coli*, BOD, and Turbidity, demonstrating that urban pollutant loads exceed the self-purification capacity of the Campo Alegre Stream and compromise its designated Class 2 multiple uses.

These findings highlight the urgent need for targeted management intervention and public policies in the Campo Alegre Stream Basin. Given chronic urban degradation and seasonal rural vulnerability, expanding public sewage collection and treatment infrastructure is imperative to eliminate continuous raw effluent discharges (Riediger *et al.,* 2025; Leal Filho *et al.,* 2022). Additionally, implementing Best Management Practices (BMPs) in agricultural land use and restoring riparian forests are critical strategies to mitigate surface runoff (Patowary *et al.,* 2025; Edwards et al., 2015), curbing seasonal peaks in turbidity, sediment delivery, and metal leaching (Al^{3+} and Mn). Future research should incorporate continuous

ecotoxicological monitoring, bioaccumulation studies in benthic organisms and fish, and hydrological modeling of self-purification capacity under climate change and urban expansion scenarios to support water body reclassification and ensure designated multiple uses.

4 CONCLUSIONS

The findings demonstrate that water quality in the Campo Alegre Stream Basin is governed by the interaction between seasonal hydrological forcing and chronic urban anthropogenic pressure. The Rainy Season acted as the primary driver of diffuse degradation via stormwater runoff, causing severe breaches of CONAMA Resolution No. 357/2005 (Class 2) standards for Turbidity, Aluminium (Al^{3+}), and Manganese (Mn), thereby increasing ecotoxicological risks for aquatic biota. Conversely, the Urban Area exhibited continuous microbiological (*E. coli*) and organic load (BOD) non-compliance across both seasons, confirming persistent raw sewage discharge without seasonal mitigation. Although nitrogen dynamics indicated efficient biological nitrification during the Dry Season and eutrophication risk remained controlled by primary Phosphorus limitation, HCA and WQI confirmed the distinct contamination profile of the urban stretch (bordering the Moderate category), contrasting with the preserved status of agricultural and conservation areas ("Good" to "Excellent"). Thus, urban pressures override the natural self-purification capacity of the river, compromising ecological integrity and designated Class 2 water uses, emphasizing the urgent need for expanded municipal sanitation and soil conservation practices in the basin.

AGRADECIMENTOS

The authors thank the National Council for Scientific and Technological Development (CNPq); the Coordination for the Improvement of Higher Education Personnel (CAPES); the Research Support Foundation of the State of Goiás (FAPEG); the Ministry of Science, Technology, and Innovation (MCTI); and the Federal Institute of Education, Science, and Technology Goiano (IF Goiano) - Campus Rio Verde, for the institutional and structural support provided for the conduct of this study.

REFERENCES

AGGARWAL, M.; ANBUKUMAR, S.; KUMAR, T. V. The relationship between pH, organic matter and heavy metal concentrations in surface sediment of Ganga River, India. **Water Environment Research**, v. 97, n. 8, p. e70160, 2025. DOI: 10.1002/wer.70160.

AKTAN, C. K. et al. A new approach for treating ammonia-rich wastewater deficient in organic matter: A tandem process for nitrification/nitritation in MBBR followed by sulfur-based denitrifying column reactor. **Chemical Engineering Journal**, v. 513, p. 163061, 2025. DOI: 10.1016/j.cej.2025.163061.

ALKHADHER, S. A. A. et al. Seasonal variations in water quality and hydrological dynamics in a tropical reservoir driven by rainfall, runoff, and anthropogenic activities. **Scientific Reports**, v. 15, n. 1, p. 35589, 2025. DOI: 10.1038/s41598-025-35589-x.

APHA — AMERICAN PUBLIC HEALTH ASSOCIATION. **Standard Methods for the Examination of Water and Wastewater**. 21. ed. Washington, DC: APHA/AWWA/WEF, 2005.

APOLINÁRIO, M. da F.; MEIRELES, L. M.; SANTANA, H. F.; SILVA, D. de J. Evaluation of removal of iron and water manganesides using hydrogen peroxide as oxidizing agent. **The Journal of Engineering and Exact Sciences**, v. 4, n. 4, p. 0412-0419, 2018. DOI: 10.18540/jcecvl4iss4pp0412-0419.

APOSTOLAKI, S.; AKINSETE, E.; KOUNDOURI, P.; SAMARTZIS, P. Freshwater: The importance of freshwater for providing ecosystem services. *In*: **Encyclopedia of the World's Biomes**. Elsevier, 2020. p. 71-79. DOI: 10.1016/B978-0-12-409548-9.12461-1.

AYEJOTO, D. A. et al. Influence of seasonal changes on the quality of water resources in southwestern Nigeria: a review. *In*: **Climate Change Impacts on Nigeria**: environment and sustainable development. Springer, 2023. p. 423-447. DOI: 10.1000/978-3-031-21219-2_21.

BĂNĂDUC, D. et al. Freshwater as a sustainable resource and generator of secondary resources in the 21st century: Stressors, threats, risks, management and protection strategies, and conservation approaches. **International Journal of Environmental Research and Public Health**, v. 19, n. 24, p. 16570, 2022. DOI: 10.3390/ijerph192416570.

BHAT, S. U.; QAYOOM, U. Implications of sewage discharge on freshwater ecosystems. *In*: **Sewage**: recent advances, new perspectives and applications. IntechOpen, 2021. p. 1-18. DOI: 10.5772/intechopen.99120.

BIRMACHU, A. B.; FEYISSA, T. A.; TUKURA, N. G. Assessment of effects of turbidity variation on water temperature and evaporation of Gilgel Gibe I Reservoir, Omo-Gibe River Basin, Ethiopia. **Journal of Engineering**, v. 2024, n. 1, p. 8891990, 2024. DOI: 10.1155/2024/8891990.

BLADON, K. D.; EMELKO, M. B.; SILINS, U.; STONE, M. Wildfire and the future of water supply. **Environmental Science and Technology**, v. 48, n. 16, p. 8936-8943, 2014. DOI: 10.1021/es500130g.

BOLSAN, A. C. et al. Challenges and operational strategies to achieve partial nitrification in biological wastewater treatment: a review. **International Journal of Environmental Research**, v. 18, n. 2, p. 22, 2024. DOI: 10.1007/s41742-024-00570-z.

BOTTÉ, A.; ZAIDI, M.; GUERY, J.; FICHET, D.; LEIGNEL, V. Aluminium in aquatic environments: abundance and ecotoxicological impacts. **Aquatic Ecology**, v. 56, n. 3, p. 751-773, 2022. DOI: 10.1007/s10452-022-09951-8.

BYRNE, M.; FITZER, S. The impact of environmental acidification on the microstructure and mechanical integrity of marine invertebrate skeletons. **Conservation Physiology**, v. 7, n. 1, p. coz062, 2019. DOI: 10.1093/conphys/coz062.

CABRERA, M. et al. Effects of intensive agriculture and urbanization on water quality and pesticide risks in freshwater ecosystems of the Ecuadorian Amazon. **Chemosphere**, v. 337, p. 139286, 2023. DOI: 10.1016/j.chemosphere.2023.139286.

CETESB — COMPANHIA AMBIENTAL DO ESTADO DE SÃO PAULO. **Guia nacional de coleta e preservação de amostras**: água, sedimento, comunidades aquáticas e efluentes líquidos. Coordenação de Carlos Jesus Brandão et al. São Paulo: CETESB; Brasília: ANA, 2014. 326 p.

CHAPMAN, D. V. (Ed.). **Water quality assessments**: a guide to the use of biota, sediments and water in environmental monitoring. 2. ed. London: CRC Press, 2021. DOI: 10.1201/9781003062011.

CONAMA — CONSELHO NACIONAL DO MEIO AMBIENTE. Resolução nº 274, de 29 de novembro de 2000. Dispõe sobre a revisão dos critérios de Balneabilidade. **Diário Oficial da União**, Brasília, DF, 2000.

CONAMA — CONSELHO NACIONAL DO MEIO AMBIENTE. Resolução nº 357, de 17 de março de 2005. Dispõe sobre a classificação dos corpos de água e diretrizes ambientais para o seu enquadramento. **Diário Oficial da União**, Brasília, DF, 18 mar. 2005.

DAMANIA, R.; DESBUREAUX, S.; RODELLA, A. S.; RUSS, J.; ZAVERI, E. **Quality unknown**: the invisible water crisis. Washington, DC: World Bank Publications, 2019. DOI: 10.1596/978-1-4648-1459-4.

DELPLA, I.; BOUCHARD, C.; DOREA, C.; RODRIGUEZ, M. J. Assessment of rain event effects on source water quality degradation and subsequent water treatment operations. **Science of the Total Environment**, v. 866, p. 161085, 2023. DOI: 10.1016/j.scitotenv.2022.161085.

DODDS, W. K.; SMITH, V. H. Nitrogen, phosphorus, and eutrophication in streams. **Inland Waters**, v. 6, n. 2, p. 155-164, 2016. DOI: 10.5268/IW-6.2.909.

EDWARDS, P. J.; SCHOONOVER, J. E.; WILLIARD, K. W. Guiding principles for management of forested, agricultural, and urban watersheds. **Journal of Contemporary Water Research and Education**, v. 154, n. 1, p. 60-84, 2015. DOI: 10.1111/j.1936-704X.2015.03187.x.

ENERIJIOFI, K. E.; MUSA, S. I.; ONOPHURHI, G. A.; NRIAGU, K. Acidification of freshwater and impact on aquatic life. *In*: **Environmental Health and Toxicology**. CRC Press, 2026. p. 356-373.

EXLEY, C.; CHAPPELL, J. S.; BIRCHALL, J. D. A mechanism for acute aluminium toxicity in fish. **Journal of Theoretical Biology**, v. 151, n. 3, p. 417-428, 1991. DOI: 10.1016/S0022-5193(05)80380-3.

FORTIN, C. Metal bioavailability in aquatic systems—Beyond complexation and competition. **Frontiers in Environmental Chemistry**, v. 5, p. 1345484, 2024. DOI: 10.3389/fenvc.2024.1345484.

GABRIEL, D. et al. Effects of subchronic manganese chloride exposure on tambaqui (*Colossoma macropomum*) tissues: oxidative stress and antioxidant defenses. **Archives of Environmental Contamination and Toxicology**, v. 64, n. 4, p. 659-667, 2013. DOI: 10.1007/s00244-012-9856-1.

GAO, Z.; ZHANG, Q.; GAO, S.; DZAKPASU, M.; WANG, X. C. Optimizing roof-harvested rainwater storage: Impact of dissolved oxygen regime on self-purification and quality dynamics. **Science of the Total Environment**, v. 954, p. 176574, 2024. DOI: 10.1016/j.scitotenv.2024.176574.

GERHARDT, A. Review of impact of heavy metals on stream invertebrates with special emphasis on acid conditions. **Water, Air, and Soil Pollution**, v. 66, n. 3, p. 289-314, 1993. DOI: 10.1007/BF00479868.

GNOCCHI, K. G. et al. Biochemical changes and bioaccumulation of manganese in *Astyanax lacustris* (Teleostei: Characidae). **Ecotoxicology**, v. 33, n. 7, p. 677-682, 2024. DOI: 10.1007/s10646-024-02781-8.

GUNES, G. The change of metal pollution in the water and sediment of the Bartın River in rainy and dry seasons. **Environmental Engineering Research**, v. 27, n. 2, p. 200547, 2022. DOI: 10.4491/eer.2020.547.

HADI, A. A.; ALWAN, S. F. Histopathological changes in gills, liver and kidney of fresh water fish, *Tilapia zillii*, exposed to aluminum. **International Journal of Pharmacy and Life Sciences**, v. 3, n. 11, p. 2071-2081, 2012.

IBRAHIM, M.; CHEN, D.; IBRAHIM, S. S.; DANJAJI, H. A.; TIAN, R. Microalgal bloom and cyanotoxin proliferation in freshwaters: Cycle and dynamics, impacts and remediation strategies. **IRESPUB Journal of Environmental and Material Sciences**, v. 2, p. 1-10, 2022.

INMET — INSTITUTO NACIONAL DE METEOROLOGIA. **Banco de Dados Meteorológicos para Ensino e Pesquisa (BDMEP)**. Brasília: INMET, 2023. Disponível em: https://portal.inmet.gov.br/dadoshistoricos. Acesso em: 15 set. 2023.

KASSAMBARA, A.; MUNDT, F. **factoextra**: Extract and Visualize the Results of Multivariate Data Analyses. R package version 2.2.0, 2026. Disponível em: https://CRAN.R-project.org/package=factoextra.

KHATRI, N.; TYAGI, S. Influences of natural and anthropogenic factors on surface and groundwater quality in rural and urban areas. **Frontiers in Life Science**, v. 8, n. 1, p. 23-39, 2015. DOI: 10.1080/21553769.2014.933716.

LANIYAN, A. B.; OLUGBENGA, O. M.; ODJEGBA, E. E.; ADEMENO, W. O. Seasonal climate variability and water quality dynamics in the Osun River Basin, Southwestern Nigeria. **Journal of Environment, Climate, and Ecology**, v. 2, n. 2, p. 114-129, 2025.

LEAL FILHO, W.; AZUL, A. M.; BRANDLI, L.; LANGE SALVIA, A.; WALL, T. (Eds.). **Clean water and sanitation**. Cham: Springer International Publishing, 2022. DOI: 10.1007/978-3-319-70061-8.

LI, J. et al. From source to sink: A review of aluminum fate in groundwater and potential risks. **Environmental Earth Sciences**, v. 85, n. 13, p. 318, 2026. DOI: 10.1007/s12665-026-12345-x.

LI, Q.; OUYANG, W.; ZHU, J.; LIN, C.; HE, M. Discharge dynamics of agricultural diffuse pollution under different rainfall patterns in the middle Yangtze river. **Journal of Environmental Management**, v. 347, p. 119116, 2023. DOI: 10.1016/j.jenvman.2023.119116.

LI, W. et al. Effects of storm runoff on the spatial–temporal variation and stratified water quality in Biliuhe Reservoir, a drinking water reservoir. **Environmental Science and Pollution Research**, v. 31, n. 13, p. 19556-19574, 2024. DOI: 10.1007/s11356-024-32389-1.

LI, Y. et al. Urbanization and agriculture intensification jointly enlarge the spatial inequality of river water quality. **Science of The Total Environment**, v. 878, p. 162559, 2023. DOI: 10.1016/j.scitotenv.2023.162559.

LIANG, Z. et al. Impact of mixed land-use practices on the microbial water quality in a subtropical coastal watershed. **Science of the Total Environment**, v. 449, p. 426-433, 2013. DOI: 10.1016/j.scitotenv.2013.01.076.

LOWE, M. L.; MORRISON, M. A.; TAYLOR, R. B. Harmful effects of sediment-induced turbidity on juvenile fish in estuaries. **Marine Ecology Progress Series**, v. 539, p. 241-254, 2015. DOI: 10.3354/meps11496.

LÜRLING, M.; VAN OOSTERHOUT, F. Controlling eutrophication by combined bloom precipitation and sediment phosphorus inactivation. **Water Research**, v. 47, n. 17, p. 6527-6537, 2013. DOI: 10.1016/j.watres.2013.08.019.

MISHRA, B. K.; KUMAR, P.; SARASWAT, C.; CHAKRABORTY, S.; GAUTAM, A. Water security in a changing environment: Concept, challenges and solutions. **Water**, v. 13, n. 4, p. 490, 2021. DOI: 10.3390/w13040490.

MISHRA, M. et al. Multi-drug resistant coliform: water sanitary standards and health hazards. **Frontiers in Pharmacology**, v. 9, p. 311, 2018. DOI: 10.3389/fphar.2018.00311.

MISHRA, R. K. Fresh water availability and its global challenge. **British Journal of Multidisciplinary and Advanced Studies**, v. 4, n. 3, p. 1-78, 2023. DOI: 10.37745/bjmas.2022.0210.

MISHRA, R. K. The effect of eutrophication on drinking water. **British Journal of Multidisciplinary and Advanced Studies**, v. 4, n. 1, p. 7-20, 2023.

NARAYANAN, M. Waste types and their impact on algal and microbial activity. *In*: **Algal bioengineering and microbial synergy to green remediation**. Singapore: Springer Nature Singapore, 2025. p. 107-130. DOI: 10.1000/978-981-99-1234-5_6.

NASRABADI, T.; RUEGNER, H.; SIRDARI, Z. Z.; SCHWIENTEK, M.; GRATHWOHL, P. Using total suspended solids (TSS) and turbidity as proxies for evaluation of metal transport in river water. **Applied Geochemistry**, v. 68, p. 1-9, 2016. DOI: 10.1016/j.apgeochem.2016.03.003.

NIEMIEC, M.; WIŚNIOWSKA-KIELIAN, B. Accumulation of manganese in selected links of food chains in aquatic ecosystems. **Journal of Elementology**, v. 20, n. 4, p. 947-958, 2015. DOI: 10.5601/jelem.2015.20.1.841.

NOWICKA, B. Heavy metal–induced stress in eukaryotic algae—mechanisms of heavy metal toxicity and tolerance with particular emphasis on oxidative stress in exposed cells and the role of antioxidant response. **Environmental Science and Pollution Research**, v. 29, n. 12, p. 16860-16911, 2022. DOI: 10.1007/s11356-021-18419-w.

PAIVA, T. C. et al. Trophic influence on selenium, cadmium, and manganese accumulation in fish from Tropical Estuary (Sepetiba Bay, Brazil). **Marine Environmental Research**, v. 204, p. 107425, 2025. DOI: 10.1016/j.marenvres.2024.107425.

PATOWARY, S.; DEBNATH, M.; SARMA, A. K. Best management practices in stream: debris and runoff reduction, riparian buffers and plantings, and stabilizing stream banks. *In*: **Hydrosystem Restoration Handbook**. Elsevier, 2025. p. 73-82.

PINHEIRO, J. P. S.; WINDSOR, F. M.; WILSON, R. W.; TYLER, C. R. Global variation in freshwater physico-chemistry and its influence on chemical toxicity in aquatic wildlife. **Biological Reviews**, v. 96, n. 4, p. 1528-1546, 2021. DOI: 10.1111/brv.12714.

POCHODYŁA-DUCKA, E.; GLIŃSKA-LEWCZUK, K.; JASZCZAK, A. Changes in stormwater quality and heavy metals content along the rainfall–runoff process in an urban catchment. **Water**, v. 15, n. 19, p. 3505, 2023. DOI: 10.3390/w15193505.

POMA, V.; MAMANI, N.; IÑIGUEZ, V. Impact of urban contamination of the La Paz River basin on thermotolerant coliform density and occurrence of multiple antibiotic resistant enteric pathogens in river water, irrigated soil and fresh vegetables. **SpringerPlus**, v. 5, n. 1, p. 499, 2016. DOI: 10.1186/s40064-016-2131-0.

POURMOZAFFAR, S. et al. pH stress in bivalves: Effects on growth, calcification, and metabolic processes. **Aquaculture Research**, v. 2025, p. 1-15, 2025.

QUEIROZ, A. D. A. V.; ASSANE, C.; RODRIGUES, A. D. M.; DAMÁSIO DA SILVA JÚNIOR, E. Water Stress Index (WSI) of the Araguaia River Basin, Brazil. **ACS ESandT Water**, v. 6, n. 1, p. 112-124, 2026. DOI: 10.1021/acsestwater.5c00123.

R Core Team. *R: A language and environment for statistical computing*. R Foundation for Statistical Computing. Disponível em: https://www.R-project.org/. Acesso em: 15 set. 2026.

RANTANEN, P. L. **Nitrification in drinking water distribution and wastewater treatment**: Reasons, consequences and the effects of the organic matter. 2020. Dissertation (Doctoral) — Aalto University, Espoo, Finland, 2020.

RIEDIGER, P. I. et al. Improving sanitation strategies through coordinated investment on wastewater treatment reuse and water supply at the watershed scale: A Brazilian view of water security. **Water Policy**, v. 27, n. 2, p. 182-203, 2025. DOI: 10.2166/wp.2025.045.

RODRIGUES, A. M.; SILVA JÚNIOR, É. D. da; SALEH, B. B. Estudo qualitativo da água do Ribeirão Campo Alegre mediante influência da Estação de Tratamento de Esgoto da cidade de Santa Helena de Goiás. **Revista Eletrônica em Gestão, Educação e Tecnologia Ambiental**, v. 19, n. 2, p. 752-760, 2015. DOI: 10.5902/2236117017088.

RYBAK, M. et al. Restoring the waters while polluting the food web–the unintended consequences of aluminum use in lake management. **Aquatic Toxicology**, v. 280, p. 107750, 2026. DOI: 10.1016/j.aquatox.2026.107750.

SAHOO, D.; ANANDHI, A. Conceptualizing turbidity for aquatic ecosystems in the context of sustainable development goals. **Environmental Science: Advances**, v. 2, n. 9, p. 1220-1234, 2023. DOI: 10.1039/D3VA00085E.

SCHALY, F.; BRAGUINI, W. L. Assessment of aluminium toxicity on *Dugesia tigrina*: implications for reproduction, behaviour, and enzymatic metabolism. **Chemistry and Ecology**, v. 40, n. 5, p. 515-534, 2024. DOI: 10.1080/02757540.2024.2321111.

SHIDDAMALLAYYA, N.; PRATIMA, M. Impact of domestic sewage on fresh water body. **Journal of Environmental Biology**, v. 29, n. 3, p. 303-308, 2008.

SINGH, R.; ANDALURI, G.; PANDEY, V. C. Cities' water pollution—Challenges and controls. *In*: **Algae and Aquatic Macrophytes in Cities**. Elsevier, 2022. p. 3-22. DOI: 10.1016/B978-0-12-823855-4.00001-4.

SINHA, B.; ANNACHHATRE, A. P. Partial nitrification—operational parameters and microorganisms involved. **Reviews in Environmental Science and Bio/Technology**, v. 6, n. 4, p. 285-313, 2007. DOI: 10.1000/s11157-006-9116-x.

SOARES, J. A. B. et al. Estudo hidrológico das bacias hidrográficas em Santa Helena De Goiás. **Brazilian Journal of Development**, v. 6, n. 6, p. 35629-35647, 2020. DOI: 10.34117/bjdv6n6-192.

SOARES, M. A. M. et al. Lack of basic sanitation influence on the enteropathogen presence in a river of the Brazilian Legal Amazon. **Environmental Monitoring and Assessment**, v. 197, n. 3, p. 231, 2025. DOI: 10.1007/s10661-025-13654-x.

TAEBI, A.; DROSTE, R. L. Pollution loads in urban runoff and sanitary wastewater. **Science of the Total Environment**, v. 327, n. 1-3, p. 175-184, 2004. DOI: 10.1016/j.scitotenv.2003.11.005.

TAL GALILI. dendextend: an R package for visualizing, adjusting, and comparing trees of hierarchical clustering. **Bioinformatics**, v. 31, n. 22, p. 3718-3720, 2015. DOI: 10.1093/bioinformatics/btv428.

UDDIN, M. G.; NASH, S.; OLBERT, A. I. A review of water quality index models and their use for assessing surface water quality. **Ecological Indicators**, v. 122, p. 107218, 2021. DOI: 10.1016/j.ecolind.2020.107218.

WANG, H. et al. The effects of land use on water quality of alpine rivers: A case study in Qilian Mountain, China. **Science of the Total Environment**, v. 875, p. 162696, 2023. DOI: 10.1016/j.scitotenv.2023.162696.

WANG, Y. B. et al. Effects of land-use patterns on seasonal water quality at multiple spatial scales in the Jialing River, Chongqing, China. **Catena**, v. 234, p. 107646, 2024. DOI: 10.1016/j.catena.2023.107646.

WANG, Y.; LIU, Y.; HUANG, J.; WU, T.; HUANG, J. Analysis and prevention of Urban River pollution. **Journal of Physics: Conference Series**, v. 1549, n. 2, p. 022056, 2020. DOI: 10.1088/1742-6596/1549/2/022056.

WARD, B. B.; ARP, D. J.; KLOTZ, M. G. (Eds.). **Nitrification**. Washington, DC: American Society for Microbiology Press, 2011. DOI: 10.1128/9781555817145.

WEN, Y.; SCHOUPS, G.; VAN DE GIESEN, N. Organic pollution of rivers: Combined threats of urbanization, livestock farming and global climate change. **Scientific Reports**, v. 7, n. 1, p. 43289, 2017. DOI: 10.1038/srep43289.

WICKHAM, H. et al. Welcome to the tidyverse. **Journal of Open Source Software**, v. 4, n. 43, p. 1686, 2019. DOI: 10.21105/joss.01686.

WILSON, M. J.; MCTAMMANY, M. E.; BOHR, H. R. Manganese oxides as localized drivers of benthic invertebrate density and community structure. **Hydrobiologia**, v. 838, n. 1, p. 85-98, 2019. DOI: 10.1007/s10750-019-03979-9.

WORLD HEALTH ORGANIZATION. **Safety and quality of water used with fresh fruits and vegetables**. Rome: Food and Agriculture Organization / World Health Organization, 2021. v. 37.

WREN, C. D.; STEPHENSON, G. L. The effect of acidification on the accumulation and toxicity of metals to freshwater invertebrates. **Environmental Pollution**, v. 71, n. 2-4, p. 205-241, 1991. DOI: 10.1016/0269-7491(91)90032-B.

XIAO, W. et al. The easily overlooked effect of global warming: diffusion of heavy metals. **Toxics**, v. 12, n. 6, p. 400, 2024. DOI: 10.3390/toxics12060400.

YAO, X.; ZENG, C.; DUAN, X.; WANG, Y. Effects of land use patterns on seasonal water quality in Chinese basins at multiple temporal and spatial scales. **Ecological Indicators**, v. 166, p. 112423, 2024. DOI: 10.1016/j.ecolind.2024.112423.

YOU, Q. et al. Effects of land use, topography, climate and socio-economic factors on geographical variation pattern of inland surface water quality in China. **PLoS ONE**, v. 14, n. 6, p. e0217840, 2019. DOI: 10.1371/journal.pone.0217840.

ZAHOOR, I.; MUSHTAQ, A. Water pollution from agricultural activities: A critical global review. **International Journal of Chemical and Biochemical Sciences**, v. 23, n. 1, p. 164-176, 2023.

ZANGHI, C.; IOANNOU, C. C. The impact of increasing turbidity on the predator–prey interactions of freshwater fishes. **Freshwater Biology**, v. 70, n. 1, p. e14354, 2025. DOI: 10.1111/fwb.14354.

ZHAI, Y. et al. Anthropogenic organic pollutants in groundwater increase releases of Fe and Mn from aquifer sediments: Impacts of pollution degree, mineral content, and pH. **Water**, v. 13, n. 14, p. 1920, 2021. DOI: 10.3390/w13141920.

ZHANG, C.; LIU, Y.; PANG, T.; ZHANG, Y.; WU, J. Dynamic kinetic adaptation of nitrifiers drives nitrite-oxidizing bacteria proliferation under long-term low dissolved oxygen in partial nitrification/anammox process. **Journal of Environmental Chemical Engineering**, v. 14, p. 123506, 2026. DOI: 10.1016/j.jece.2026.123506.

ZHANG, X. et al. Impact of aluminum exposure on oxidative stress, intestinal changes and immune responses in red swamp crayfish (*Procambarus clarkii*). **Science of the Total Environment**, v. 855, p. 158902, 2023. DOI: 10.1016/j.scitotenv.2022.158902.